COVECTIVE HEAT AND MASS TRANSFER FLOW IN A CYLINDRICAL ANNULUS WITH CHEMICAL REACTION, SORET AND DUFOUR EFFECTS

B. Haritha
[1]Department of Mathematics, Santhiram Engineering College,Nandyal, (A.P.), India.

R. Bhuvana Vijaya
Department of Mathematics,
J. N. T. U. A Engineering College, Anantapuram, (A.P.), India.

Dr. D. R. V. Prasada Rao
Department of Mathematics
Retired Professor in S. K. University
Anantapuram, (A.P.), India.

ABSTRACT: We discuss the effect of thermo-diffusion and diffusion-thermo on non-Darcy convective heat and mass transfer flow of a viscous, electrically conducting fluid through a porous medium in a Co-axial cylindrical duct where the boundaries are maintained at temperature Tw and Concentration Cw. The behavior of velocity, temperature and concentration is analyzed at different axial positions. The shear stress and the rate of heat and mass transfer have also been obtained for variations in the governing parameters.

KEY WORDS: Cylindrical Annulus, Soret Effect, Dufour Effect, Chemical Reaction, Heat and Mass Transfer, Non-darcy, Porous Medium.

I. INTRODUCTION:

Thermal-diffusion (soret effect) and diffusion-thermo(dufour effect) have been found to appreciably effect in a rotating channel, in a vertical channel and ducts, in rotating system and in a vertical porous plate with various effects such as chemical reaction, heat source, dissipation, magnetic field and radiation under various conditions. Many researchers and academicians alike advanced their studies in analyzing the influence of thermal-diffusion and diffusion-thermo, among others, are Adrian Postelnicu et al [1], Sreevani et al [2], Barletta [3] and Zanchini et al [4], Indudhar et al [5], Madhusudhan Reddy et al [6], Kamalakar et al [7], Rajasekhar et al [8], Muthucumaraswamy et al [9], Jafarunnisa et al [10], Alam et al [11], Kafoussias and Williams et al [12], Alam et al [13], Alam et al [14], Lakshminarayana et al [15], Naga Radhika et al [16], Dulal pal et al [17], Ching-Yang-Cheng et al [18], Dulal pal et al [19], Sulochana and Tayappa et al [20], Ramana Reddy et al [21], Raju et al [22], Raju et al [23], Raju et al [24].

The free convection with conceivable three-dimensional and transient effects and radial magnetic field in a horizontal and vertical porous annulus has been analyzed by Leppinen et al (25), Jha et al (26), Saravanan and Kandaswamy et al (27), Charrier Mojtabi et al (28), Chmaissem et al (29), Sivanjaneya Prasad et al (30). Neeraja et al (31) investigated the fluid flow and the heat transfer in a viscous incompressible fluid enclosed by two rigid cylinders maintained in an annulus. Antonio et al (32) analyzed the heat transfer in a vertical cylinder duct by considering buoyancy effect and viscous dissipation within the laminar flow. The natural convection in the porous annulus is solved analytically for steady and transient cases was analyzed by Sharawi and Al-Nimir et al (33), Al-Nimir et al (34). Chamkha et al [35] have studied the influence of radiation on heat and mass transfer by non-Darcy natural convection in a porous medium. Prasad et al (36) discussed the impact of a radial magnetic field on convective heat and mass transfer in an annulus.

The influence of Soret effect on mixed convective heat and mass transfer during a porous cylindrical annulus was analyzed by Sreenivasa Reddy et al (37). Sudheer Kumar et al (38) analyzed the effect of radiation on natural convection over a vertical cylinder in a porous media. Padmavathi et al (39) concentrated the convective heat transfer in a cylindrical annulus by using finite element technique. Madhusudhan Reddy et al (40) researched the convective heat and mass transfer flow of a viscous fluid through a porous medium in a vertical cylindrical annulus with constant temperature and concentration. The influence of soret and dufour effect in different fluid and in various shapes like concentric cylindrical annulus, vertical cylindrical annulus and circular cylindrical annulus with various parameters and varied conditions was studied with utmost keenness by Sudarsana Reddy et al (41,42), Mallikarjuna et al (43), Srinivasa Reddy et al (44), Sulochana et al (45).

In this paper we discuss the effect of thermo-diffusion and diffusion-thermo on non-Darcy convective heat and mass transfer flow of a viscous, electrically conducting fluid through a porous medium in a Co-axial cylindrical duct where the boundaries are maintained at temperature Tw and Concentration Cw. The behavior of velocity, temperature and concentration is analyzed at different axial positions. The shear stress and the rate of heat and mass transfer have also been obtained for variations in the governing parameters.

II. FORMULATION OF THE PROBLEM:

We recall the free and forced convection at fixed temperature and concentration in a vertical circular annulus through a porous medium. We considered the temperature

21

and concentration are fully developed in the entire flow. Both the fluid and permeable area have steady physical characteristics and the stream is a mixed convection stream adopting thermal and molecular buoyancies and constant axial pressure gradient. A uniform radial magnetic field is applied. The Boussinesq approximation is considered facilitating the density confinement to the molecular buoyancy and thermal buoyancy forces. The Brinkman-Forchheimer-Extended Darcy model based on the influence of inertia and boundary effects is applied for the momentum equation in the permeable area. We consider the momentum, energy and diffusion equations are coupled and non-linear. The stream is unidirectional along the axial direction of the cylindrical annulus. Making utilization of the above assumptions the governing equations are

$$-\frac{\partial p}{\partial z}+\frac{v}{\delta}\left(\frac{\partial^2 u}{\partial r^2}+\frac{1}{r}\frac{\partial u}{\partial r}\right)-\left(\frac{v}{k}\right)u-\frac{\sigma\mu_e^2 H_0^2}{r^2}-\frac{\delta F}{\sqrt{k}}u^2+\rho\beta(T-T_i)+\rho\beta^*(C-C_i)=0 \quad (1)$$

$$\rho C_p u\frac{\partial T}{\partial z}=k_f\left(\frac{\partial^2 T}{\partial r^2}+\frac{1}{r}\frac{\partial T}{\partial r}\right)+Q_H(T-T_0)+\frac{D_m K_T}{C_s C_p}\left(\frac{\partial^2 C}{\partial r^2}+\frac{1}{r}\frac{\partial C}{\partial r}\right) \quad (2)$$

$$u\frac{\partial C}{\partial z}=D_m\left(\frac{\partial^2 C}{\partial r^2}+\frac{1}{r}\frac{\partial C}{\partial r}\right)-k_c'C+\frac{D_m K_T}{T_s}\left(\frac{\partial^2 T}{\partial r^2}+\frac{1}{r}\frac{\partial T}{\partial r}\right) \quad (3)$$

Where u, T, C, p, δ, k, σ, μ_e, H_0, F, ρ, β, $\boldsymbol{\beta^*}$, C_p, k_f, Q_H, D_m, K_T are defined in the nomenclature section.
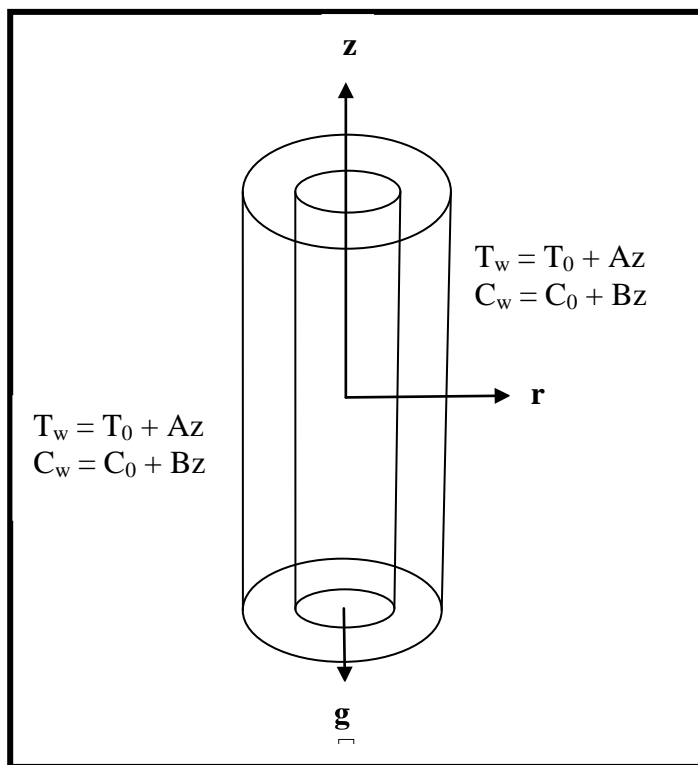
Fig: CONFIGURATION OF THE PROBLEM

The relevant boundary conditions are

$u = 0$, T=T_w, C=C_w at   r = a & a+s   (4)

Following Tao(46),we assume that the temperature and concentration of the both walls is $T_w = T_0 + Az$, $C_w = C_0 + Bz$ where A and B   are the vertical temperature and concentration gradients which are positive for buoyancy–aided flow and negative for buoyancy–opposed flow, respectively, T_0 and C_0 are the upstream reference wall temperature and concentration, respectively. For the fully developed laminar flow in the presences of radial magnetic field, the velocity depend only on the radial coordinate and all the other physical variables except temperature, concentration and pressure are functions of r and z, z being the vertical co-ordinate. The temperature and concentration inside the fluid can be written as

$$T = T^{\bullet}(r) + Az \quad , \quad C = C^{\bullet}(r) + Bz \tag{5}$$

We now define the following non-dimensional variables

$$z^* = \frac{z}{a} \quad , \quad r^* = \frac{r}{a} \quad , \quad u^* = (\frac{a}{v})u$$

$$p^* = \frac{pa\delta}{\rho v^2} \quad , \quad \theta^*(r^{\bullet}) = \frac{T^{\bullet} - T_0}{Aa} \quad , \quad C^*(r^{\bullet}) = \frac{C^{\bullet} - C_0}{Ba} \quad , \quad , \quad s^* = \frac{s}{a}$$

Introducing these non-dimensional variables, the governing equations in the non-dimensional form are (on removing the stars)

$$(\frac{\partial^2 u}{\partial r^2} + \frac{1}{r}\frac{\partial u}{\partial r}) = 1 + \delta(D^{-1} + \frac{M^2}{r^2})u + \delta^2 (D^{-1})^{1/2}\Delta u^2 - \delta G(\theta + NC) \tag{6}$$

$$(\frac{\partial^2 \theta}{\partial r^2} + \frac{1}{r}\frac{\partial \theta}{\partial r}) = \Pr u + \alpha\theta + Du\Pr(\frac{\partial^2 C}{\partial r^2} + \frac{1}{r}\frac{\partial C}{\partial r}) \tag{7}$$

$$(\frac{\partial^2 C}{\partial r^2} + \frac{1}{r}\frac{\partial C}{\partial r}) - \gamma C = Sc\,u + ScSr\left(\frac{\partial^2 \theta}{\partial r^2} + \frac{1}{r}\frac{\partial \theta}{\partial r}\right) \tag{8}$$

Where

$\Delta = FD^{-1}$ (Inertia parameter or Forchheimer number)

$G = \dfrac{g\beta(T_e - T_i)a^3}{v^2}$ (Grashof number) $\quad D^{-1} = \dfrac{a^2}{k}$ (Inverse Darcy parameter)

$M^2 = \dfrac{\sigma\mu_e^2 H_0^2}{av}$ (Hartmann number) $\quad P_r = \dfrac{\mu C_p}{k_f}$ (Prandtl number)

$Sc = \dfrac{v}{D_m}$ (Schmidt number) $\quad S_r = \dfrac{D_m K_T A}{T_s B}$ (Soret Parameter)

$Du = \dfrac{D_b K_T B}{C_s C_p A}$ (Dufour parameter) $\quad \alpha = \dfrac{Q_H a^2}{k_f}$ (Heat source parameter)

$\gamma = \dfrac{k_c^1 a^2}{D_B}$ (Chemical Reaction parameter)

The corresponding non-dimensional conditions are

$$u = 0, \ \theta = 0, \ C=0 \quad \text{at} \ \ r=1 \text{ and } 1+s \tag{9}$$

III. FINITE ELEMENT ANALYSIS:

Using the finite element analysis with quadratic polynomial approximation functions is done along the radial distance across the circular duct. For the varied parameters, we analyzed computationally the velocity, temperature and concentration profiles with various variations. The Gelarkin method has been choose in the variational formulation in every element to get the global coupled matrices for the velocity, temperature and concentration in course of the finite element analysis.

Choose an arbitrary element e_k and let u^k, θ^k and C^k be the values of u, θ and C in the element e_k.

We define the error residuals as

$$E_u^k = \frac{d}{dr}\left(r\frac{du^k}{dr}\right) + \delta G(\theta^k) - \delta(D^{-1} + \frac{M^2}{r^2})ru^k - \delta^2 \Delta r(u^k)^2 \tag{10}$$

$$E_\theta^k = \frac{1}{\Pr} \frac{d}{dr}\left(r\frac{d\theta^k}{dr} \right) - ru^k + \frac{\alpha}{P_r} r\theta + Du\frac{d}{dr}\left(r\frac{d^{\,k}}{dr} \right) \quad (11)$$

$$E_c^k = \frac{d}{dr}\left(r\frac{d^{\,k}}{dr} \right)C - rScu^k - \gamma\, C^k + ScSr\frac{d}{dr}\left(r\frac{d\theta^k}{dr} \right) \quad (12)$$

Where u^k, θ^k & C^k are v du s o f u , θ& C in the arbitrary element e_k. These are expressed as linear combinations in terms of respective local nodal values.

$$u^k = u_1^k \psi_1^k + u_2^k \psi_1^k + u_3^k \psi_3^k$$

$$\theta^k = \theta_1^k \psi_1^k + \theta_2^k \psi_2^k + \theta_3^k \psi_3^k$$

$$C^k = C_1^k \psi_1^k + C_2^k \psi_2^k + C_3^k \psi_3^k$$

Where ψ_1^k, ψ_2^k, --------- etc are Lagrange's quadratic polynomials.

Following the Gelarkin weighted residual method and integrating by parts, the equations (10) - (12) becomes

We obtain

$$\int_{rA_1}^{rB_1} r\frac{du^k}{dr}\frac{d\psi_j^k}{dr}dr - \delta G\int_{rA_1}^{rB_1} r(\theta^k)\psi_j^k dr + \delta(M_1^2)\int_{rA_1}^{rB_1} ru^k\psi_j^k dr + \delta^2\Delta\int_{rA_1}^{rB_1} r(u^k)^2\psi_j^k dr$$

$$= Q_{2\,j}^k + Q_{1\,j}^k - P\int_{rA_1}^{rB_1} r\psi_j^k dr \quad (13)$$

$$-Q_{1\,j}^k = \left[\left(\frac{du^k}{dr}\right)(r\psi_j^k)\right]r_{A_1} \quad , \quad -Q_{2\,j}^k = \left[\left(\frac{du^k}{dr}\right)(r\psi_j^k)\right]r_{B_1}$$

$$\int_{rA_1}^{rB_1} r\frac{d\theta^k}{dr}\frac{d\psi_j^k}{dr}dr + \alpha\int_{rA_1}^{rB_1} r\theta^k dr + Du\int_{rA_1}^{rB_1} r\frac{dC^k}{dr}\frac{d\psi_j^k}{dr}dr - P_r\int_{rA_1}^{rB_1} ru^k\psi_j^k dr + R_{2\,j}^k + R_{1\,j}^k \quad (14)$$

$$-R_{1\,j}^k = \left[\left(\frac{d\theta^k}{dr}\right)(r\psi_j^k)\right]r_{A_1} \quad , \quad R_{2\,j}^k = \left[\left(\frac{d\theta^k}{dr}\right)(r\psi_j^k)\right]r_{B_1}$$

$$\int_{rA_1}^{rB_1} r\frac{dC^k}{dr}\frac{d\psi_j^k}{dr}dr - \gamma\int_{rA_1}^{rB_1} rC^k dr = Sc\int_{rA_1}^{rB_1} ru^k\psi_j^k dr + ScSr\int_{rA_1}^{rB_1} r\frac{d\theta^k}{dr}\frac{d\psi_j^k}{dr}dr + S_{2\,j}^k + S_{1\,j}^k \quad (15)$$

$$-S_{1\,j}^k = \left[\left(\frac{dC^k}{dr}\right)(r\psi_j^k)\right]r_{A_1} \quad , \quad S_{2\,j}^k = \left[\left(\frac{dC^k}{dr}\right)(r\psi_j^k)\right]r_{B_1}$$

Expressing u^k, θ^k, C^k in terms of local nodal values in (13) - (14).

We obtain

$$\sum_{i=1}^{3} u_i^k \int_{rA_1}^{rB_1} r \frac{d\psi_i^k}{dr} \frac{d\psi_j^k}{dr} dr - \delta G \sum_{i=1}^{3} (\theta_i^k) \int_{rA_1}^{rB_1} r\psi_i^k \psi_j^k dr + \frac{1}{A_1 A_3} \delta(D^{-1}) \sum_{i=1}^{3} \int_{rA_1}^{rB_1} r\psi_i^k \psi_j^k dr$$

$$+ M^2 \sum_{i=1}^{3} \int_{rA_1}^{rB_1} ((1/r)\psi_i^k \psi_j^k dr) + \delta^2 \Delta \sum_{i=1}^{3} u_i^k \int_{rA_1}^{rB_1} rU_i^k \psi_i^k \psi_j^k dr = Q_{2\,j}^j + Q_{1\,j}^k - P \int_{rA_1}^{rB_1} r\psi_i^k \psi_j^k dr \tag{16}$$

$$\frac{1}{\text{Pr}} \sum_{i=1}^{3} \theta_i^k \int_{rA_1}^{rB_1} r \frac{d\psi_i^k}{dr} \frac{d\psi_j^k}{dr} dr - \sum_{i=1}^{3} u_i^k \int_{rA_1}^{rB_1} r\psi_i^k \psi_j^k dr + Du \sum_{i=1}^{3} C_i^k \int_{rA_1}^{rB_1} r \frac{d\psi_i^k}{dr} \frac{d\psi_j^k}{dr} dr +$$

$$\alpha \sum_{i=1}^{3} \theta_i^k \int_{rA_1}^{rB_1} r\psi_i^k \psi_j^k dr = R_{2\,j}^k + R_{1\,j}^k \tag{17}$$

$$\sum_{i=1}^{3} C_i^k \int_{rA_1}^{rB_1} r \frac{d\psi_i^k}{dr} \frac{d\psi_j^k}{dr} dr - \gamma \sum_{i=1}^{3} C_i^k \int_{rA_1}^{rB_1} r\psi_i^k \psi_j^k dr + Sc \sum_{i=1}^{3} u_i^k \int_{rA_1}^{rB_1} r\psi_i^k \psi_j^k dr +$$

$$+ ScSr \sum_{i=1}^{3} \theta_i^k \int_{rA_1}^{rB_1} r \frac{d\psi_i^k}{dr} \frac{d\psi_j^k}{dr} dr = S_{2\,j}^k + S_{1\,j}^k \tag{18}$$

Choosing different ψ_j^k's corresponding to each element e_k in the equation (16) yields a local stiffness matrix

of order 3×3 in the form

$$(f_{i\,j}^k)(u_i^k) - \delta G(g_{i\,j}^k)(\theta_i^k) + \delta D^{-1}(m_{i\,j}^k)(u_i^k) +$$
$$\delta M^2 (m_{i\,j}^k)(u_i^k) + \delta^2 \Delta(n_{i\,j}^k)(u_i^k) = (Q_{2\,j}^k) + (Q_{1\,j}^k) + (v_j^k) \tag{19}$$

Likewise the equation (17) & (18) give rise to stiffness matrices

$$(e_{i\,j}^k)(\theta_i^k) + \alpha(f_{i\,j}^k)(\theta_i^k) - (t_{i\,j}^k)(u_i^k) + Du(p_{i\,j}^k)(C_i^k) = R_{2\,j}^k + R_{1\,j}^k \tag{20}$$

$$(l_{i\,j}^k - \gamma)(C_i^k) - ScSr(t_{i\,j}^k) = S_{2\,j}^k + S_{1\,j}^k \tag{21}$$

Where $(f_{i\,j}^k)$, $(g_{i\,j}^k)$, $(m_{i\,j}^k)$, $(n_{i\,j}^k)$, $(e_{i\,j}^k)$, $(l_{i\,j}^k)$, $(p_{i\,j}^k)$, $(r_{i\,j}^k)$ and $(t_{i\,j}^k)$ are 3×3 matrices and

$v_j^k = -P_1 \int_{rA_1}^{rB_1} r\psi_i^k \psi_j^k dr$ and $(Q_{2\,j}^k)$, $(Q_{1\,j}^k)$, $(R_{2\,j}^k) \& (R_{1\,j}^k)$, $(S_{2\,j}^k)$ & $(S_{1\,j}^k)$ are 3×1 column matrices. By

utilizing inter element continuity and equilibrium conditions; those stiffness matrices (10) - (12) are collected in every element of local nodes to achieve the coupled global matrices with regard to the global nodal values of u, θ & C in the area.

Suppose we select n quadratic elements, then the global matrices are defined in order 2n+1. To evaluate the unknown global nodal values of the concentration, temperature and velocity, we find final coupled global matrices in fluid area. In an iteration process we solve these global matrices by involving the boundary effects in the permeable strata.

Actuality, the non-linear term emerges in the modified Brinkman linear momentum equation (4) of the porous medium. We split the square term into a product term and keeping one of them say U_i's under integration, the

another term is expanded in terms of local nodal values as in (7), resulting in the corresponding coefficient matrix $(n_{i\,j}^k\,'s)$ in

(10), whose coefficients involve the unknown U_i's . To calculate (10), to start with, select the initial global nodal values of U_i's as zeros in the zeroth approximation. We evaluate u_i's, θ_i's and C_i's in the usual procedure. Afterward selecting these values of u_i's as first order approximation calculate θ_i's, C_i's. In the second iteration, we replacement for U_i's the first order approximation of and u_i's and the first approximation of θ_i's and C_i's and get second order approximation. This process is continued till the successive values of u_i's , θ_i's and C_i's change by a pre assigned percentage.
For computational purpose we choose five elements in flow region.
The shape functions in the region are

$$\psi_1^1 = \frac{50(-1 + r - \frac{s}{5})(-1 + r - \frac{s}{10})}{s^2} \quad , \quad \psi_2^1 = \frac{100(-1 + r)(-1 + r - \frac{s}{5})}{s^2}$$

$$\psi_3^1 = \frac{50(-1 + r)(-1 + r - \frac{s}{10})}{s^2} \quad , \quad \psi_1^2 = \frac{50(-1 + r - \frac{2s}{5})(-1 + r - \frac{3s}{10})}{s^2}$$

$$\psi_2^2 = -\frac{100(-1 + r - \frac{2s}{5})(-1 + r - \frac{s}{5})}{s^2} \quad , \quad \psi_3^2 = \frac{50(-1 + r - \frac{3s}{5})(-1 + r - \frac{s}{5})}{s^2}$$

$$\psi_1^3 = \frac{50(-1 + r - \frac{3s}{5})(-1 + r - \frac{s}{2})}{s^2} \quad , \quad \psi_2^3 = -\frac{100(-1 + r - \frac{3s}{5})(-1 + r - \frac{2s}{5})}{s^2}$$

$$\psi_3^3 = \frac{50(-1 + r - \frac{s}{2})(-1 + r - \frac{2s}{5})}{s^2} \quad , \quad \psi_1^4 = \frac{50(-1 + r - \frac{4s}{5})(-1 + r - \frac{7s}{10})}{s^2}$$

$$\psi_2^4 = -\frac{100(-1 + r - \frac{4s}{5})(-1 + r - \frac{3s}{5})}{s^2} \quad , \quad \psi_3^4 = \frac{50(-1 + r - \frac{7s}{10})(-1 + r - \frac{3s}{5})}{s^2}$$

$$\psi_1^5 = \frac{50(-1 + r - s)(-1 + r - \frac{9s}{10})}{s^2} \quad , \quad \psi_2^5 = -\frac{100(-1 + r - s)(-1 + r - \frac{4s}{5})}{s^2}$$

$$\psi_3^5 = \frac{50(-1 + r - \frac{9s}{10})(-1 + r - \frac{4s}{5})}{s^2}$$

IV. SOLUTION OF THE PROBLEM:

By using an iteration process, solving these coupled global matrices for temperature, concentration and velocity respectively. We evaluate the unknown global nodes at different radial intervals at any arbitrary axial cross sections. The respective expressions are given by

$$\theta(r) = \psi_1^1 \theta_{11} + \psi_{21}^1 \theta_{12} + \psi_3^1 \theta_{13} \qquad 1 \le r \le 1 + S*0.2$$

$$= \psi_1^2 \theta_{13} + \psi_2^2 \theta_{14} + \psi_3^2 \theta_{15} \qquad 1 + S*0.2 \le r \le 1 + S*0.4$$

$$= \psi_1^3 \theta_{15} + \psi_2^3 \theta_{16} + \psi_3^3 \theta_{17} \qquad 1 + S*0.4 \le r \le 1 + S*0.6$$

$$= \psi_1^4 \theta_{17} + \psi_2^4 \theta_{18} + \psi_3^4 \theta_{19} \qquad 1 + S*0.6 \le r \le 1 + S*0.8$$

$$= \psi_1^{15} \theta_{19} + \psi_2^5 \theta_{20} + \psi_3^5 \theta_{21} \qquad 1 + S*0.8 \le r \le 1 + S$$

$$C(r) = \psi_1^1 C_{11} + \psi_{21}^1 C_{12} + \psi_3^1 C_{13} \qquad 1 \le r \le 1 + S*0.2$$

$$= \psi_1^2 C_{13} + \psi_2^2 C_{14} + \psi_3^2 C_{15} \qquad 1 + S*0.2 \le r \le 1 + S*0.4$$

$$= \psi_1^3 C_{15} + \psi_2^3 C_{16} + \psi_3^3 C_{17} \qquad 1 + S*0.4 \le r \le 1 + S*0.6$$

$$= \psi_1^4 C_{17} + \psi_2^4 C_{18} + \psi_3^4 C_{19} \qquad 1 + S*0.6 \le r \le 1 + S*0.8$$

$$= \psi_1^{15} C_{19} + \psi_2^5 C_{20} + \psi_3^5 C_{21} \qquad 1 + S*0.8 \le r \le 1 + S$$

$$u(r) = \psi_1^1\, u_{11} + \psi_{21}^1\, u_{12} + \psi_3^1\, u_{13} \qquad 1 \le r \le 1+S*0.2$$

$$= \psi_1^2\, u_{13} + \psi_2^2\, u_{14} + \psi_3^2\, u_{15} \qquad 1+S*0.2 \le r \le 1+S*0.4$$

$$= \psi_1^3\, c_{15} + \psi_2^3\, c_{16} + \psi_3^3\, c_{17} \qquad 1+S*0.4 \le r \le 1+S*0.6$$

$$= \psi_1^4\, u_{17} + \psi_2^4\, u_{18} + \psi_3^4\, u_{19} \qquad 1+S*0.6 \le r \le 1+S*0.8$$

$$= \psi_1^{15}\, u_{19} + \psi_2^5\, u_{20} + \psi_3^5\, u_{21} \qquad 1+S*0.8 \le r \le 1+S$$

(A) STIFFNESS MATRICES:

The global matrix for

θ is $\qquad A_3 X_3 = B_3$

C is $\qquad A_4 X_4 = B_4$

u is $\qquad A_5 X_5 = B_5$

Where

A3 =

$$\begin{pmatrix}
1 & \frac{4}{3}+\frac{2s}{75} & -\frac{1}{3}-\frac{s}{75} & 0 & 0 & 0 & 0 & 0 & 0 & 0 & 0 \\[4pt]
0 & -\frac{4s}{75} & \frac{4}{3}+\frac{7s}{75} & 0 & 0 & 0 & 0 & 0 & 0 & 0 & 0 \\[4pt]
0 & -\frac{4}{3}-\frac{8s}{75} & -\frac{2s}{75} & \frac{4}{3}+\frac{4s}{25} & -\frac{1}{3}-\frac{7s}{150} & 0 & 0 & 0 & 0 & 0 & 0 \\[4pt]
0 & 0 & -\frac{4}{3}-\frac{13s}{75} & -\frac{4s}{75} & \frac{4}{3}+\frac{17s}{75} & 0 & 0 & 0 & 0 & 0 & 0 \\[4pt]
0 & 0 & \frac{1}{3}+\frac{4s}{75} & -\frac{4}{3}-\frac{6s}{25} & -\frac{2s}{75} & \frac{4}{3}+\frac{22s}{75} & -\frac{1}{3}-\frac{2s}{25} & 0 & 0 & 0 & 0 \\[4pt]
0 & 0 & 0 & 0 & -\frac{4}{3}-\frac{23s}{75} & -\frac{4s}{75} & \frac{4}{3}+\frac{9s}{25} & 0 & 0 & 0 & 0 \\[4pt]
0 & 0 & 0 & 0 & \frac{1}{3}+\frac{13s}{150} & -\frac{4}{3}-\frac{28s}{75} & -\frac{2s}{75} & \frac{4}{3}+\frac{32s}{75} & -\frac{1}{3}-\frac{17s}{150} & 0 & 0 \\[4pt]
0 & 0 & 0 & 0 & 0 & 0 & -\frac{4}{3}-\frac{11s}{25} & -\frac{4s}{75} & \frac{4}{3}+\frac{37s}{75} & 0 & 0 \\[4pt]
0 & 0 & 0 & 0 & 0 & 0 & \frac{1}{3}+\frac{3s}{25} & -\frac{4}{3}-\frac{38s}{75} & -\frac{2s}{75} & \frac{4}{3}+\frac{14s}{25} & -\frac{1}{3}-\frac{11s}{75} \\[4pt]
0 & 0 & 0 & 0 & 0 & 0 & 0 & 0 & -\frac{4}{3}-\frac{43s}{75} & -\frac{4s}{75} & \frac{4}{3}+\frac{47s}{75} \\[4pt]
0 & 0 & 0 & 0 & 0 & 0 & 0 & 0 & \frac{1}{3}+\frac{23s}{150} & -\frac{4}{3}-\frac{16s}{25} & 1+\frac{73s}{150}
\end{pmatrix}$$

A4 =

$$\begin{pmatrix}
-1 & \frac{2}{3}-\frac{20}{3s} & -\frac{1}{6}+\frac{10}{3s} & 0 & 0 & 0 & 0 & 0 & 0 & 0 & 0 \\[4pt]
0 & -\frac{8}{3}-\frac{80}{3s} & 2+\frac{40}{3s} & 0 & 0 & 0 & 0 & 0 & 0 & 0 & 0 \\[4pt]
0 & -2-\frac{20}{3s} & \frac{4}{3}+\frac{20}{3s} & -\frac{2}{3}-\frac{20}{3s} & \frac{1}{2}+\frac{10}{3s} & 0 & 0 & 0 & 0 & 0 & 0 \\[4pt]
0 & 0 & \frac{10}{3}+\frac{40}{3s} & -8-\frac{80}{3s} & \frac{14}{3}+\frac{40}{3s} & 0 & 0 & 0 & 0 & 0 & 0 \\[4pt]
0 & 0 & \frac{3}{2}+\frac{10}{3s} & -\frac{10}{3}-\frac{20}{3s} & \frac{8}{3}+\frac{20}{3s} & -2-\frac{20}{3s} & \frac{7}{6}+\frac{10}{3s} & 0 & 0 & 0 & 0 \\[4pt]
0 & 0 & 0 & 0 & 6+\frac{40}{3s} & -\frac{40}{3}-\frac{80}{3s} & \frac{22}{3}+\frac{40}{3s} & 0 & 0 & 0 & 0 \\[4pt]
0 & 0 & 0 & 0 & \frac{13}{6}+\frac{10}{3s} & -\frac{14}{3}-\frac{20}{3s} & 4+\frac{20}{3s} & -\frac{10}{3}-\frac{20}{3s} & \frac{11}{6}+\frac{10}{3s} & 0 & 0 \\[4pt]
0 & 0 & 0 & 0 & 0 & 0 & \frac{26}{3}+\frac{40}{3s} & -\frac{56}{3}-\frac{80}{3s} & 10+\frac{40}{3s} & 0 & 0 \\[4pt]
0 & 0 & 0 & 0 & 0 & 0 & \frac{17}{6}+\frac{10}{3s} & -6-\frac{20}{3s} & \frac{16}{3}+\frac{20}{3s} & -\frac{14}{3}-\frac{20}{3s} & 0 \\[4pt]
0 & 0 & 0 & 0 & 0 & 0 & 0 & 0 & \frac{34}{3}+\frac{40}{3s} & -24-\frac{80}{3s} & 0 \\[4pt]
0 & 0 & 0 & 0 & 0 & 0 & 0 & 0 & \frac{7}{2}+\frac{10}{3s} & \frac{22}{3}-\frac{20}{3s} & -1
\end{pmatrix}$$

$$A_5 = \begin{pmatrix} -1 & b_{1,2} & b_{1,3} & 0 & 0 & 0 & 0 & 0 & 0 & 0 & 0 \\ 0 & b_{2,2} & b_{2,3} & 0 & 0 & 0 & 0 & 0 & 0 & 0 & 0 \\ 0 & b_{3,2} & b_{3,3} & b_{3,4} & b_{3,5} & 0 & 0 & 0 & 0 & 0 & 0 \\ 0 & 0 & b_{4,3} & b_{4,4} & b_{4,5} & 0 & 0 & 0 & 0 & 0 & 0 \\ 0 & 0 & b_{5,3} & b_{5,4} & b_{5,5} & b_{5,6} & b_{5,7} & 0 & 0 & 0 & 0 \\ 0 & 0 & 0 & 0 & b_{6,5} & b_{6,6} & b_{6,7} & 0 & 0 & 0 & 0 \\ 0 & 0 & 0 & 0 & b_{7,5} & b_{7,6} & b_{7,7} & b_{7,8} & b_{7,9} & 0 & 0 \\ 0 & 0 & 0 & 0 & 0 & 0 & b_{8,7} & b_{8,8} & b_{8,9} & 0 & 0 \\ 0 & 0 & 0 & 0 & 0 & 0 & b_{9,7} & b_{9,8} & b_{9,9} & b_{9,10} & 0 \\ 0 & 0 & 0 & 0 & 0 & 0 & 0 & 0 & b_{10,9} & b_{10,10} & 0 \\ 0 & 0 & 0 & 0 & 0 & 0 & 0 & 0 & b_{11,9} & b_{11,10} & -1 \end{pmatrix}$$

$$h_{i,j} = f_{i,j} + \delta D^{-1} m_{i,j} + \delta^2 \Delta n_{i,j}$$

$$X_3 = \begin{bmatrix} \theta_1 \\ \theta_2 \\ \theta_3 \\ \theta_4 \\ \theta_5 \\ \theta_6 \\ \theta_7 \\ \theta_8 \\ \theta_9 \\ \theta_{10} \\ \theta_{11} \end{bmatrix} \quad X_4 = \begin{bmatrix} C_1 \\ C_2 \\ C_3 \\ C_4 \\ C_5 \\ C_6 \\ C_7 \\ C_8 \\ C_9 \\ C_{10} \\ C_{11} \end{bmatrix} \quad X_5 = \begin{bmatrix} u_1 \\ u_2 \\ u_3 \\ u_4 \\ u_5 \\ u_6 \\ u_7 \\ u_8 \\ u_9 \\ u_{10} \\ u_{11} \end{bmatrix} \quad B_4 = \begin{bmatrix} c_{1,1} \\ c_{2,1} \\ c_{3,1} \\ c_{4,1} \\ c_{5,1} \\ c_{6,1} \\ c_{7,1} \\ c_{8,1} \\ c_{9,1} \\ c_{10,1} \\ c_{11,1} \end{bmatrix} \quad B_5 = \begin{bmatrix} d_{1,1} \\ d_{2,1} \\ d_{3,1} \\ d_{4,1} \\ d_{5,1} \\ d_{6,1} \\ d_{7,1} \\ d_{8,1} \\ d_{9,1} \\ d_{10,1} \\ d_{11,1} \end{bmatrix}$$

$$
B3 = \left\{
\begin{array}{l}
\dfrac{m\,s\,\alpha_1}{10\,(4+3\,m)} + \dfrac{50\,ap\,N_t\left(\frac{s^3}{3750}v_{12} - \frac{s^3}{7500}v_{13} - \frac{s^4}{75000}v_{13}\right)}{s^2} \\[2ex]
\dfrac{300\,m\left(-\frac{s^3}{750} - \frac{s^4}{7500}\right)\alpha_1}{(4+3\,m)\,s^2} - \dfrac{100\,ap\,N_t\left(-\frac{2s^3}{1875}v_{12} - \frac{s^4}{9375}v_{12} - \frac{s^3}{7500}v_{13} - \frac{s^4}{37500}v_{13}\right)}{s^2} \\[2ex]
-\dfrac{300\,m\left(\frac{s^3}{1500} + \frac{s^4}{7500}\right)\alpha_1}{(4+3\,m)\,s^2} + \dfrac{50\,ap\,N_t\left(\frac{s^3}{3750}v_{12} + \frac{s^4}{18750}v_{13} + \frac{s^3}{1875}v_{13} + \frac{7s^4}{75000}v_{13}\right)}{s^2} + \dfrac{50\,ap\,N_t\left(\frac{s^3}{1875}v_{13} + \frac{3s^4}{25000}v_{13} + \frac{s^3}{3750}v_{14} + \frac{s^4}{18750}v_{14} + \frac{s^3}{7500}v_{15} - \frac{s^4}{25000}v_{15}\right)}{s^2} \\[2ex]
-\dfrac{300\,m\left(-\frac{s^3}{750} - \frac{s^4}{2500}\right)\alpha_1}{(4+3\,m)\,s^2} - \dfrac{100\,ap\,N_t\left(-\frac{s^3}{7500}v_{13} - \frac{s^4}{37500}v_{13} - \frac{2s^3}{1875}v_{14} - \frac{s^4}{3125}v_{14} - \frac{s^3}{7500}v_{15} - \frac{s^4}{18750}v_{15}\right)}{s^2} \\[2ex]
-\dfrac{300\,m\left(\frac{s^3}{1500} + \frac{s^4}{3750}\right)\alpha_1}{(4+3\,m)\,s^2} + \dfrac{50\,ap\,N_t\left(\frac{s^3}{7500}v_{13} - \frac{s^4}{25000}v_{13} + \frac{s^3}{3750}v_{14} - \frac{s^4}{9375}v_{14} + \frac{s^3}{1875}v_{15} - \frac{s^4}{5000}v_{15}\right)}{s^2} + \dfrac{50\,ap\,N_t\left(\frac{s^3}{1875}v_{15} + \frac{17s^4}{75000}v_{15} + \frac{s^3}{3750}v_{16} - \frac{s^4}{9375}v_{16} + \frac{s^3}{7500}v_{17} - \frac{s^4}{15000}v_{17}\right)}{s^2} \\[2ex]
-\dfrac{300\,m\left(-\frac{s^3}{750} - \frac{s^4}{1500}\right)\alpha_1}{(4+3\,m)\,s^2} - \dfrac{100\,ap\,N_t\left(-\frac{s^3}{7500}v_{15} - \frac{s^4}{18750}v_{15} - \frac{2s^3}{1875}v_{16} - \frac{s^4}{1875}v_{16} - \frac{s^3}{7500}v_{17} - \frac{s^4}{12500}v_{17}\right)}{s^2} \\[2ex]
-\dfrac{300\,m\left(\frac{s^3}{1500} + \frac{s^4}{2500}\right)\alpha_1}{(4+3\,m)\,s^2} + \dfrac{50\,ap\,N_t\left(-\frac{s^3}{7500}v_{15} - \frac{s^4}{15000}v_{15} + \frac{s^3}{3750}v_{16} - \frac{s^4}{6250}v_{16} + \frac{s^3}{1875}v_{17} + \frac{23s^4}{75000}v_{17}\right)}{s^2} + \dfrac{50\,ap\,N_t\left(\frac{s^3}{1875}v_{17} + \frac{s^4}{3000}v_{17} + \frac{s^3}{3750}v_{18} + \frac{s^4}{6250}v_{18} + \frac{s^3}{7500}v_{19} - \frac{7s^4}{75000}v_{19}\right)}{s^2} \\[2ex]
\dfrac{300\,m\left(-\frac{s^3}{750} - \frac{7s^4}{7500}\right)\alpha_1}{(4+3\,m)\,s^2} - \dfrac{100\,ap\,N_t\left(-\frac{s^3}{7500}v_{17} - \frac{s^4}{12500}v_{17} - \frac{2s^3}{1875}v_{18} - \frac{7s^4}{9375}v_{18} - \frac{s^3}{7500}v_{19} - \frac{s^4}{9375}v_{19}\right)}{s^2} \\[2ex]
-\dfrac{300\,m\left(\frac{s^3}{1500} + \frac{s^4}{1875}\right)\alpha_1}{(4+3\,m)\,s^2} + \dfrac{50\,ap\,N_t\left(-\frac{s^3}{7500}v_{17} - \frac{7s^4}{75000}v_{17} + \frac{s^3}{3750}v_{18} + \frac{2s^4}{9375}v_{18} + \frac{s^3}{1875}v_{19} + \frac{31s^4}{75000}v_{19}\right)}{s^2} + \dfrac{50\,ap\,N_t\left(\frac{s^3}{1875}v_{19} + \frac{11s^4}{25000}v_{19} + \frac{s^3}{3750}v_{20} + \frac{2s^4}{9375}v_{20}\right)}{s^2} \\[2ex]
\dfrac{300\,m\left(-\frac{s^3}{750} - \frac{3s^4}{2500}\right)\alpha_1}{(4+3\,m)\,s^2} - \dfrac{100\,ap\,N_t\left(-\frac{s^3}{7500}v_{19} - \frac{s^4}{9375}v_{19} - \frac{2s^3}{1875}v_{20} - \frac{3s^4}{3125}v_{20}\right)}{s^2} \\[2ex]
-\dfrac{150\,m\left(\frac{s^3}{1500} + \frac{s^4}{1500}\right)\alpha_1}{(4+3\,m)\,s^2} + \dfrac{50\,ap\,N_t\left(-\frac{s^3}{7500}v_{19} - \frac{3s^4}{25000}v_{19} + \frac{s^3}{3750}v_{20} + \frac{s^4}{3750}v_{20}\right)}{s^2}
\end{array}
\right\}
$$

The equilibrium conditions are

$$R_3^1 + R_1^2 = 0, \qquad R_3^2 + R_1^3 = 0, \qquad R_3^3 + R_1^4 = 0, \qquad R_3^4 + R_1^5 = 0,$$

$$Q_3^1 + Q_1^2 = 0, \qquad Q_3^2 + Q_1^3 = 0, \qquad Q_3^3 + Q_1^4 = 0, \qquad Q_3^4 + Q_1^5 = 0,$$

$$S_3^1 + S_1^2 = 0, \qquad S_3^2 + S_1^3 = 0, \qquad S_3^3 + S_1^4 = 0, \qquad S_3^4 + S_1^5 = 0,$$

(B) SHEAR STRESS, NUSSELT NUMBER AND SHERWOOD NUMBER:

The shear stress (τ) is evaluated using the formula $\qquad \tau = (\dfrac{du}{dr})_{r=1,1+s}$

The rate of heat transfer (Nusselt number) is evaluated using the formula $Nu = -(\dfrac{d\theta}{dr})_{r=1,1+s}$

The rate of mass transfer (Sherwood number) is evaluated using the formula $Sh = -(\dfrac{dC}{dr})_{r=1,1+s}$

V. COMPARISON TABLE:

In the absence of Dufour effect (Du=0) the results of stress, Nusselt number and Sherwood number on the inner and outer cylinders r=1 &r=2 are found to be in good agreement with Neeraja et al (47), (2016).

CONFERENCE PAPER
National Conference dated 27-28 July 2017 on
Recent Advances in Graph Theory and its Applications (NCRAGTA2017)
Organized by Dept of Applied Mathematics
Sri Padmawati Mahila Vishvavidyalayam (Women's University) Tirupati, A.P.,
India

Results of Neeraja et al (2016)

	τ(1)	τ(2)	Nu(1)	Nu(2)	Sh(1)	Sh(2)
N						
0.5	-0.1502	0.27719	0.40572	6.2736	1.36734	1.3003
1.5	-0.1503	0.28231	0.40573	6.2739	0.93006	9.2278
-0.5	-0.1519	0.27208	0.40571	6.2719	-1.10566	30.284
-1.5	-0.1501	0.26696	0.40569	6.2706	-2.81328	19.756
Sr/Du						
0.75	-0.1502	0.27719	0.405725	6.27366	1.36734	-1.3003
1	-0.1542	0.43784	0.405727	6.27361	3.84034	-32.8846
1.5	-0.1552	0.47800	0.405729	6.27355	4.45859	-40.7807
γ						
0.5	-0.1502	0.27719	0.405728	6.2736	1.36734	-1.3003
1.5	-0.1493	0.30907	0.405724	6.2731	1.35678	-1.8740
-0.5	-0.1505	0.38579	0.405699	6.2728	1.36075	-3.4152
-1.5	-0.1452	0.25495	0.405722	6.2735	1.31638	-0.5125

Present results (Du=0):

	τ(1)	τ(2)	Nu(1)	Nu(2)	Sh(1)	Sh(2)
N						
0.5	-0.1499	0.27718	0.40571	6.2737	1.36735	1.3006
1.5	-0.1501	0.28229	0.40572	6.2740	0.93008	9.2279
-0.5	-0.1517	0.27198	0.40570	6.2718	-1.10567	30.286
-1.5	-0.1503	0.26678	0.40569	6.2705	-2.81329	19.755
Sr/Du						
0.75	-0.1499	0.277159	0.40571	6.2737	1.36735	-1.3006
1	-0.1540	0.437839	0.40572	6.2736	3.84033	-32.884
1.5	-0.1549	0.477999	0.40573	6.2735	4.45856	-40.781
γ						
0.5	-0.1499	0.27718	0.40571	6.2737	1.36735	-1.3005
1.5	-0.1490	0.30905	0.40572	6.2733	1.35679	-1.8743
-0.5	-0.1502	0.38576	0.40569	6.2729	1.36074	-3.4154
-1.5	-0.1450	0.25494	0.40572	6.2736	1.31639	-0.5126

VI. RESULTS AND DISCUSSION:

Keeping in mind the end goal to get physical insights of knowledge into the problem, we have completed numerical calculations for non-dimensional velocity, temperature and spices concentration, skin-friction, Nusselt number and Sherwood number by allotting some particular values to the parameters entering into the problem

Effect of parameters on velocity profiles:

Fig.1 displays the variation of the velocity at any point in the flow region enhances with increase in the buoyancy parameter (G). It is found that the axial velocity (u) is vertically downwards (u<0) is the actual flow and u>0 represents the reversed flow. The maximum of u occurs at r=1 and 2. The axial velocity increases with increase in G. Fig.2 represents u with Hartmann number (M). The axial velocity decreases with increase in M. This is because of the way that when the magnetic field is applied in the radial direction, the ponder motive force acts in the upward direction to depreciates the fluid velocity. Fig.3 shows the variation of velocity u with inverse Darcy parameter D^{-1}. It is seen that increasing the values D^{-1} decreases the primary and secondary velocities owing to the fact that the presence of porous medium increases the resistance to the flow resulting in the reduction of velocity of fluid. Fig.4 exhibits the variation of u with heat source parameter (α). An enhancement in the strength of the heat generating source (α>0) smaller the velocity. Fig.5 demonstrates the variation of velocity u with Schmidt number (Sc), it is find that the velocity increases with increments in Sc. This is because of the fact that increasing Sc means reducing molecular diffusivity. Therefore the molecular diffusivity is smaller for the higher velocity. Fig.6 exhibits the variation of velocity u with

buoyancy ratio (N). It is noticed that when the molecular buoyancy force dominates over the thermal buoyancy force the axial velocity enhances irrespective of the directions of the buoyancy forces. The effect of chemical reaction parameter (γ) on u is shown in fig.7. It is found that the axial velocity increases in the degenerating chemical reaction case (γ>0) and in the generating chemical reaction case the velocity decreases in magnitude. Fig.8 represents the velocity u with Soret and Dufour parameter. An enhancement of Soret parameter (Sr) (or decreasing Dufour parameter Du) increases the axial velocity. Fig.9 exhibits the variation of u with Forchheimer number (Δ). An increase in Δ enhances the velocity. This is due to the fact that increasing Δ decreases the momentum boundary layer of the channel.

Effect of parameters on temperature profiles:

The non-dimensional temperature (θ) is appeared in figs.10-18 for various parametric representation. We follow the convention that the non-dimensional temperature (θ) is positive/negative according as the actual temperature (T^*) is greater/lesser than the reference temperature (T_0). Fig.10 shows the temperature with increase in G. The actual temperature enhances except in the region (-0.2, 0.2) where it reduces with increment in Grashof number with maximum attained at r=1.5. The variation of θ with Hartmann number (M) demonstrates that higher the Lorentz force lesser the actual temperature in the fluid region except in the central region (-0.2, 0.2) where it increases with M (fig.11). Fig.12 exhibits the variation of temperature θ with inverse Darcy parameter D^{-1}. It can be seen from figures that lesser the permeability of the porous medium smaller the actual temperature except it increases in (-0.2, 0.2). Fig.14 displays the variation of θ with Sc, it shows lesser the molecular diffusivity smaller the actual temperature except it enhances in the region (-0.2, 0.2). Fig.15 represents the variation of θ with buoyancy ratio (N), when the buoyancy forces are in the same direction and for the forces acting in opposite directions the actual temperature depreciates, except it reduces with N>0 and increases with N<0 in the central region (-0.2, 0.2). Fig.13 represents the variation of θ with heat source parameter (α). It is observed from the profiles that an increase in the strength of the heat generating source leads depreciation in the actual temperature, except it enhances in the central region(-0.2,0.2). Fig.16 exhibits the variation of θ with chemical reaction parameter (γ). From the profiles we find that the actual temperature enhances with increase in γ in the degenerating chemical reaction case and depreciates in the generating chemical reaction case. Fig.17 shows the variation of θ with Sr and Du. An increasing Sr (or decreasing Du) leads to an enhancement in the actual concentration while it depreciates in the region (-0.2, 0.2). Fig.18 represents the variation of θ with Forchheimer number (Δ). As the Forchheimer number enhances there is a significant decrease in the thermal boundary layer with a fall in the actual temperature throughout the flow region, since increment of Δ amounts to depreciation of thermal diffusion, except in the central core region(-0.2,0.2) where it increases.

Effect of parameters on concentration profiles:

The non-dimensional concentration (C) is exhibits in figs.19-27 for various parametric variations. We follow the convention that the non-dimensional concentration (C) is positive/negative according as the actual concentration (C^*) is greater/lesser than the reference concentration (C_0). Fig.19 represents the variation of Concentration C with Grashof number G. It can be observed from the profiles that the actual concentration increases in the central region (-0.2, 0.2) while it enhances in regions adjoining the boundaries r=1&2 with increasing G. Fig.20 shows the variation of concentration C with M. Higher the Lorentz force larger the actual concentration while it depreciates in the region (-0.2, 0.2). This is because of the way that increase in M enhances the thickness of concentration boundary layer. Fig.21 displays the variation of C with inverse Darcy parameter D^{-1}. The actual concentration increases in the regions adjacent to the boundaries r=1&2, except it decreases in the central region (-0.2, 0.2). Fig.22 represents the variation of C with heat source parameter (α). An increase in α>0, enhances the actual concentration in the regions adjoining to r=1&2 while it depreciates in the central region (-0.2, 0.2). Fig.23 displays the variation of concentration C with Sc. The actual concentration decreases in the regions adjacent to the boundaries while it enhances in (-0.2, 0.2) with increase in Sc. In this manner the molecular diffusivity is lesser and the actual concentration is smaller. This is due to the fact that an enhancement in Schmidt number depreciates the thickness of the concentration boundary layer. Fig.24 expresses the variation of C with buoyancy ratio N. The actual concentration reduces with N>0 in the flow region adjoining the boundaries while it enhances in (-0.2, 0.2) when the buoyancy forces are in the same direction and for the forces acting in opposite directions a reversed effect is observed in the actual concentration. Fig.25 exhibits the variation of concentration C with Chemical reaction parameter (γ). The actual concentration depreciates in the degenerating chemical reaction case while in the generating chemical reaction case we noticed an increment in the actual concentration in the flow regions adjacent to r=1&2 while a reversed effect is noticed in the actual concentration in the central region (-0.2, 0.2). Fig.26 represents the variation of concentration with Soret and Dufour parameters. It is seen from the profiles that increasing Sr (or decreasing Du) leads to reduction in the actual concentration while it reduces in the central region (-0.2, 0.2). Fig.27 displays the variation of C with Forchheimer number (Δ). As the Forchheimer number enhances there is a marginal depreciation in the actual concentration in the regions adjoining to r=1&2 while it increases in the central flow region. This is due to the fact the increment of Forchheimer number amounts to reduction of thermal diffusion.

Effects of parameters on Skin friction, Nusselt number and Sherwood number:

The Skin friction, the rate of heat and mass transfer on the internal and external cylinder r=1&2 are represented in table.1. From the tabular values we find that an increase in G enhances the skin friction on both the cylinders. An increase in M or D^{-1} enhances the skin friction on both the cylinders. The variation of τ with Sc exhibits that lesser the molecular diffusivity larger the skin friction on both the cylinders. When the molecular buoyancy force dominates over the thermal buoyancy force the skin friction increases on r=1 &2 irrespective of the directions of the buoyancy forces. With reference to the chemical reaction parameter (γ) we find that the skin friction increases in the degenerating chemical reaction case and decreases in the generating

chemical reaction case on both cylinders. With reference to the Soret and Dufour parameters we find that enhancing Soret parameter (or decreasing Dufour parameter Du) increases the skin friction on r=1 & 2. As the Prandtl number increases, the skin friction also increases on r=1 and 2.

The Nusselt number increases with enhancement in G or Δ while Nu depreciates with M or Sc or D^{-1} on both the cylinders. With respect to the chemical reaction parameter (γ), the magnitude of Nu on r=1 enhances and that on r=2 reduces in the degenerating chemical reaction case while in the generating chemical reaction case it increases on both the cylinders. The rate of heat transfer enhances on r=1 and depreciates on r=2 when the buoyancy forces are in the same direction and for the forces acting in opposite directions, Nu decreases on both the cylinders. Increasing Sr(or decreasing Du) leads to an enhancement in Nu on both the cylinders. |Nu| with Δ demonstrates that lesser the thermal diffusivity larger the rate of heat transfers on r=1 and 2.

The Sherwood number enhances with increment in G and depreciates on r=1&2 with increase in M & D^{-1}. An increase in Sc enhances Sh on r=2 and decreases on r=1. An increase in the strength of the heat generating source depreciates Sh on r=1&2. As for the chemical reaction parameter (γ), |Sh| increases on both cylinders in the degenerating chemical reaction case while in the generating chemical reaction case it depreciates on both cylinders. When the molecular buoyancy force dominates over the thermal buoyancy force |Sh| enhances on r=1 and r=2 when the buoyancy forces are in the same direction and for the forces acting in opposite directions it reduces on internal and external cylinders. Enhancing Sr(or decreasing Du) leads to an increment in Sh on both the cylinders. As the Forchheimer number (Δ) increases we observed an enhancement in Sh on r=1 &2.

VII. GRAPHS:
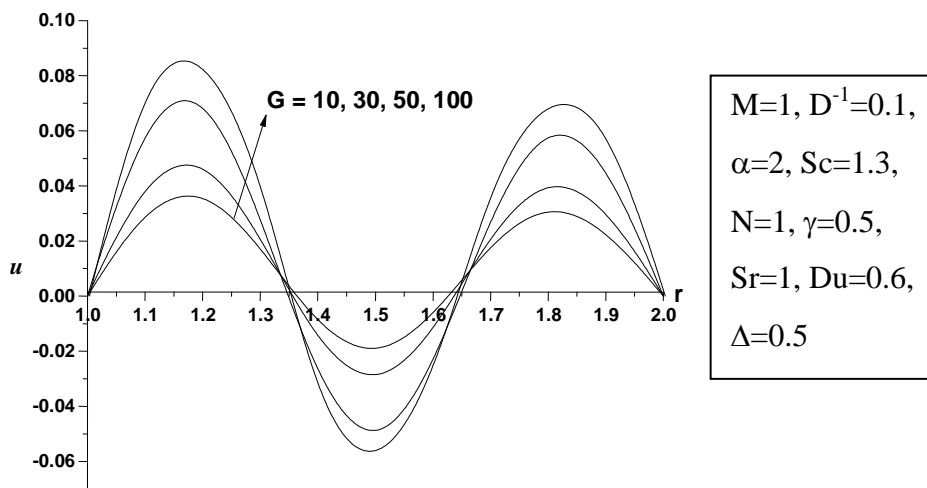
Fig.1: Variation of velocity (u) with Grashof number (G)
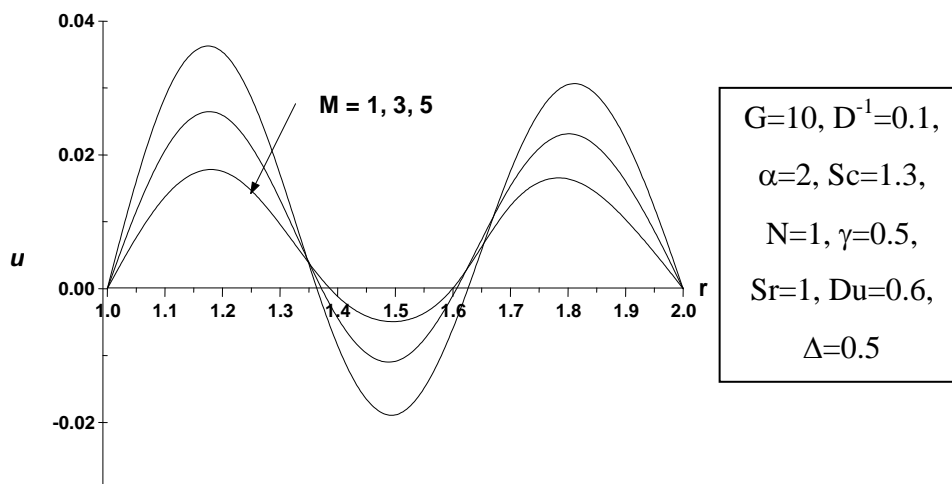
Fig.2: Variation of velocity (u) with Hartmann number (M)
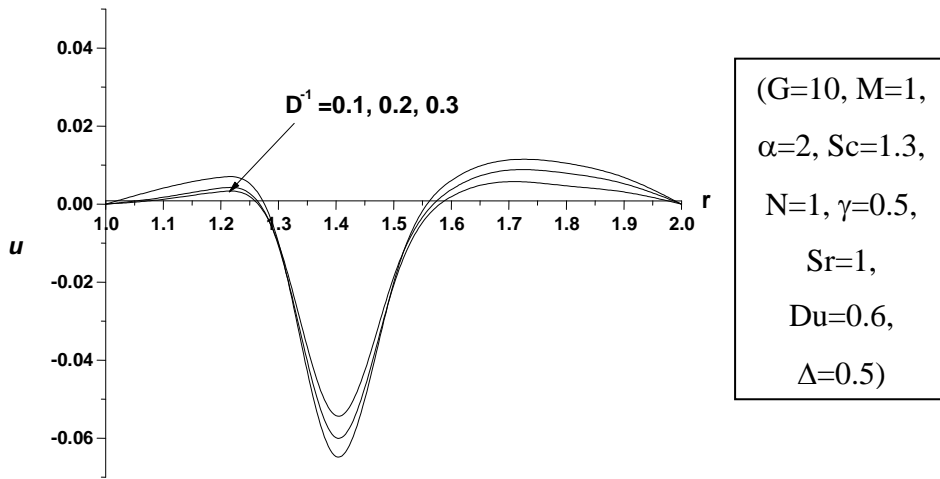
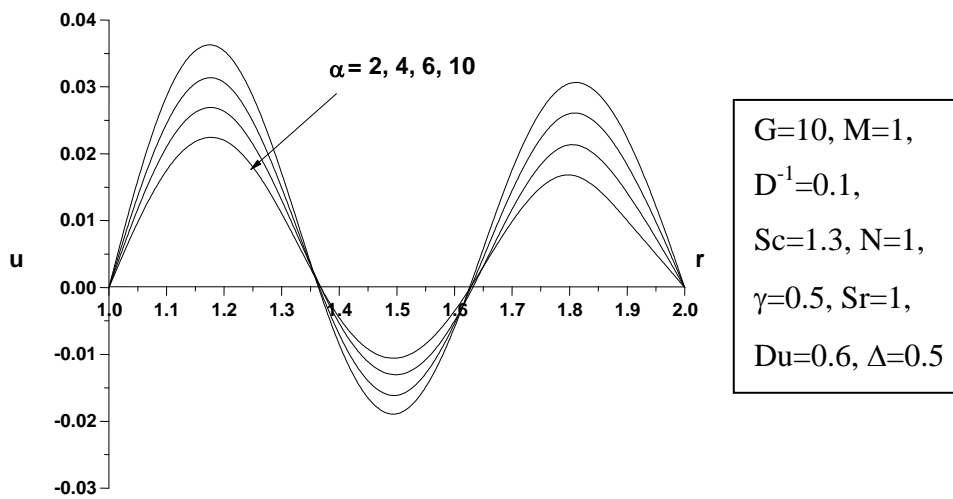Fig.3: Variation of velocity (u) with Darcy parameter (D^{-1})

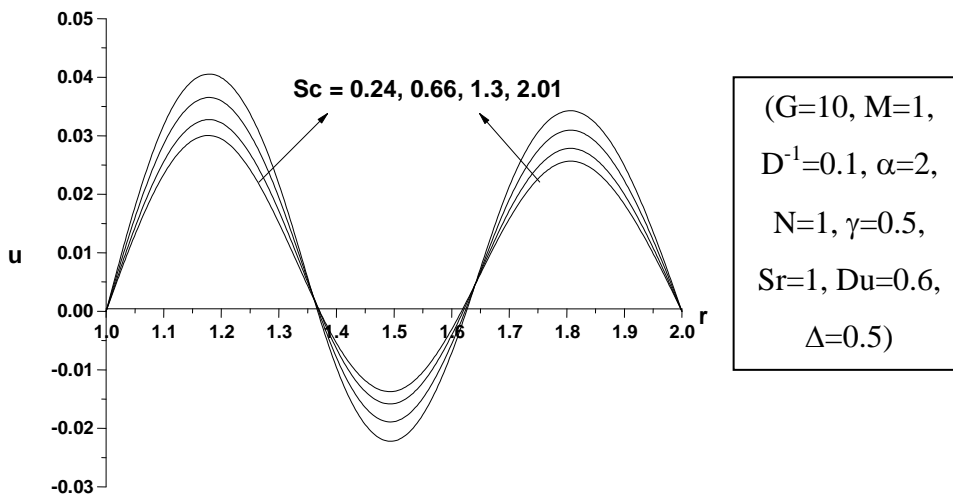Fig.4: Variation of velocity (u) with Heat source parameter (α)

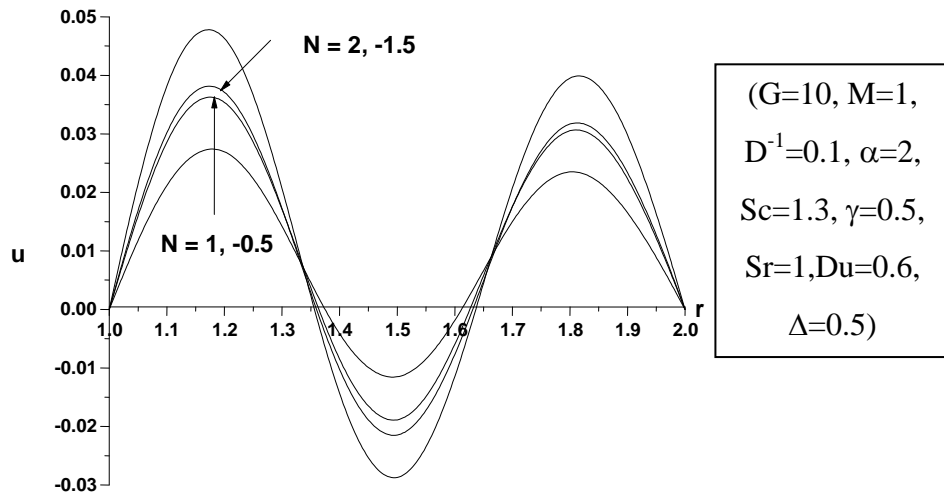Fig.5: Variation of velocity (u) with Schmidt number (Sc)

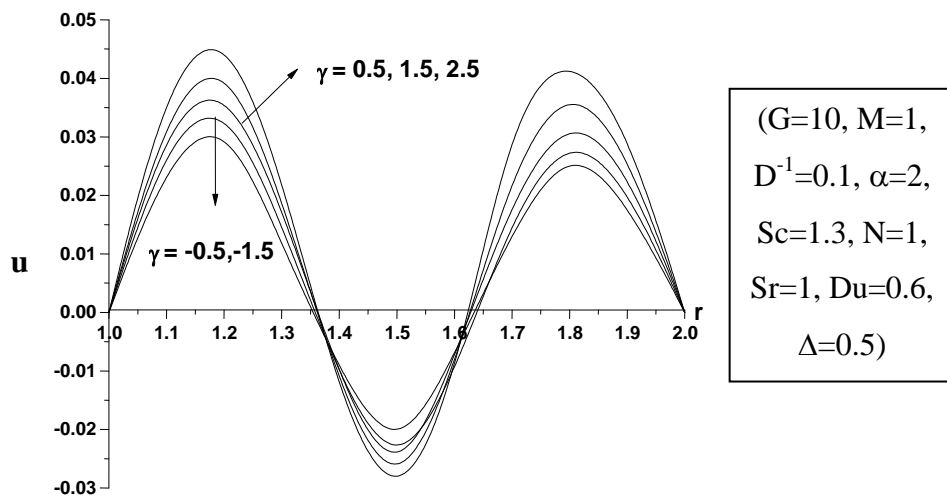Fig.6: Variation of velocity (*u*) with Buoyancy number N

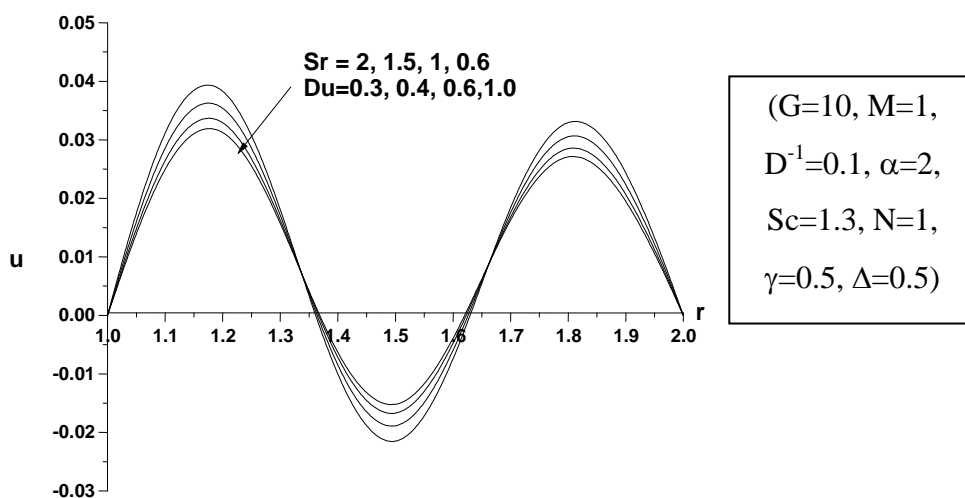Fig.7: Variation of velocity *u* with Chemical reaction parameter γ

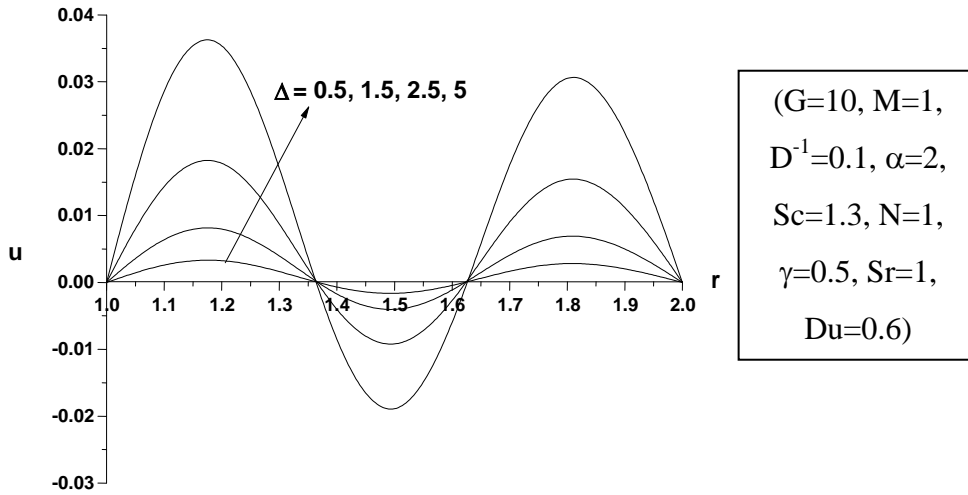Fig. 8: Variation of velocity *u* with Soret and Dufour Sr/Du
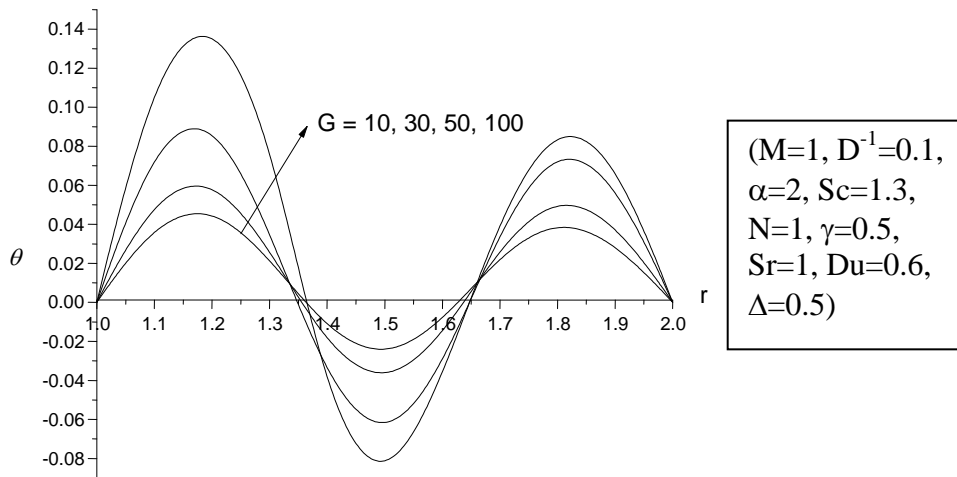
Fig. 9: Variation of velocity *u* with Forchheimer number Δ

Fig. 10: Variation of temperature θ with Grashof number G
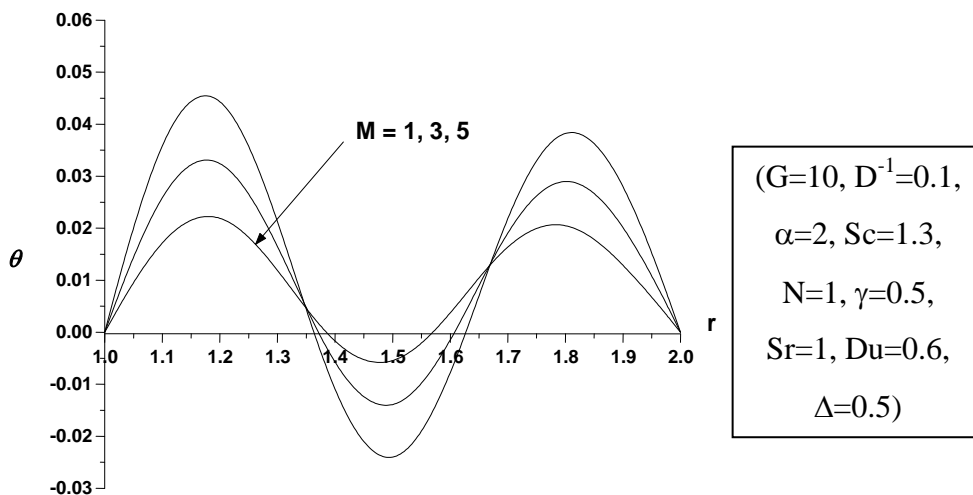
Fig. 11: Variation of temperature θ with Hartmann number M

35
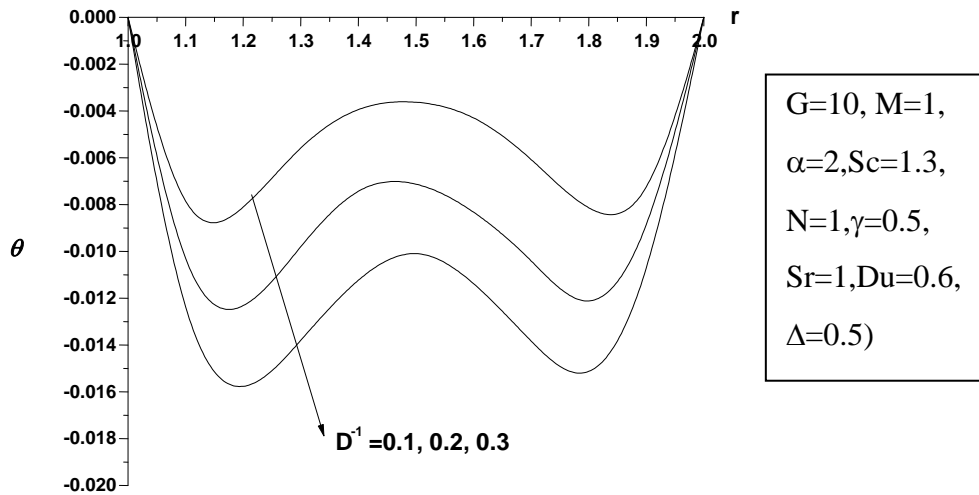
Fig. 12: Variation of temperature θ with Darcy parameter D^{-1}
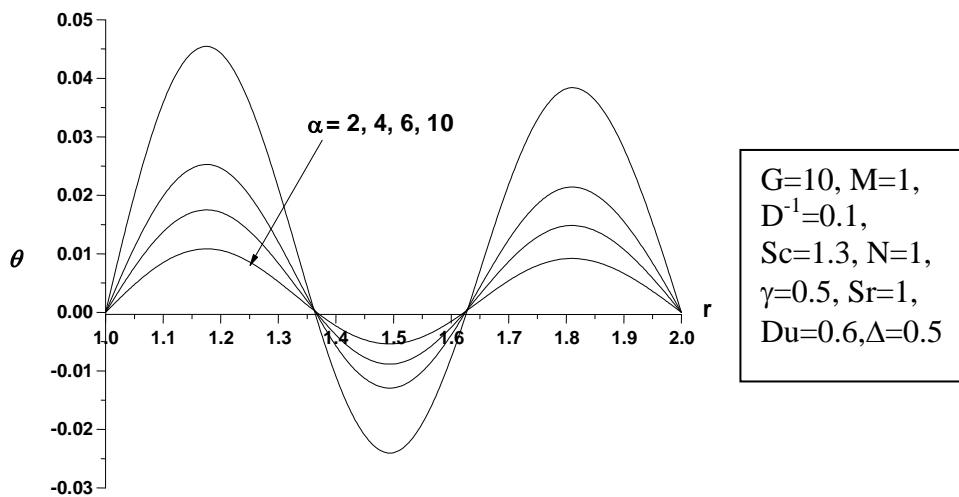
Fig. 13: Variation of temperature θ with Heat source parameter α
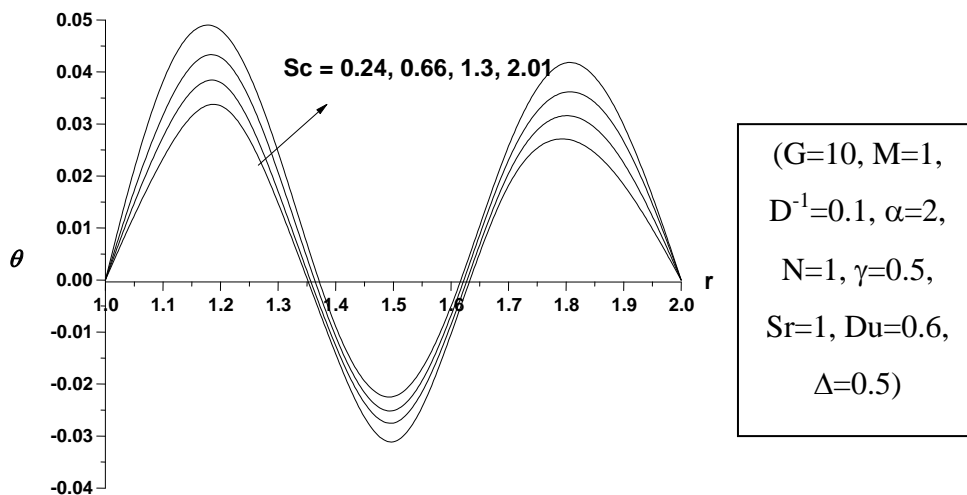
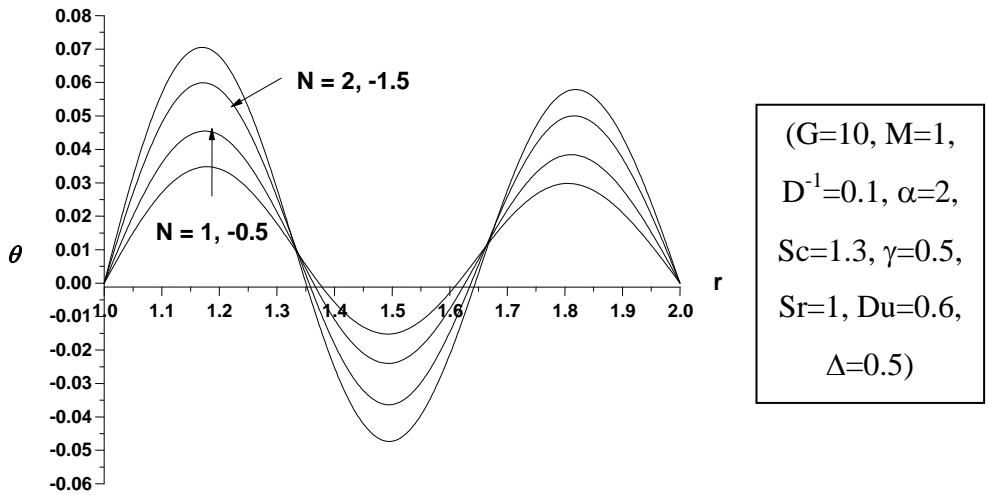Fig. 14: Variation of temperature θ with Schmidt number Sc

Fig. 15: Variation of temperature θ with Buoyancy ratio N
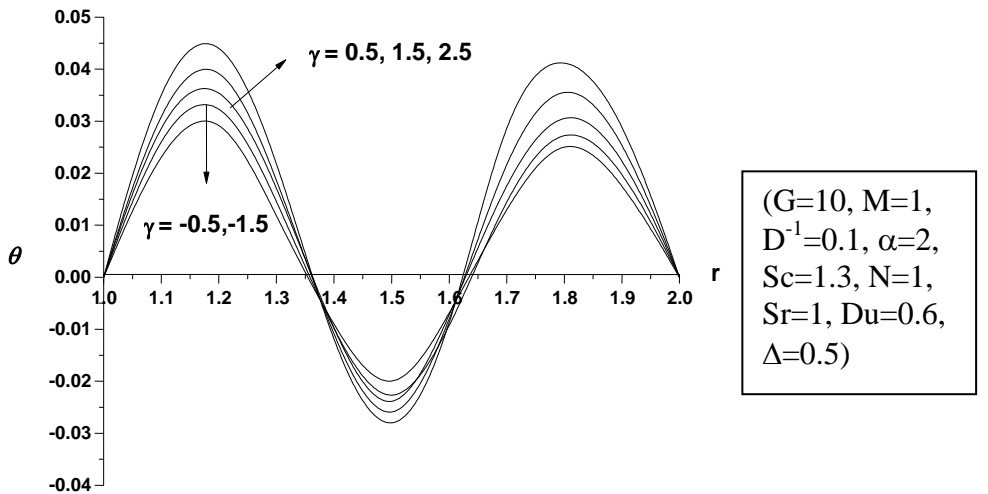

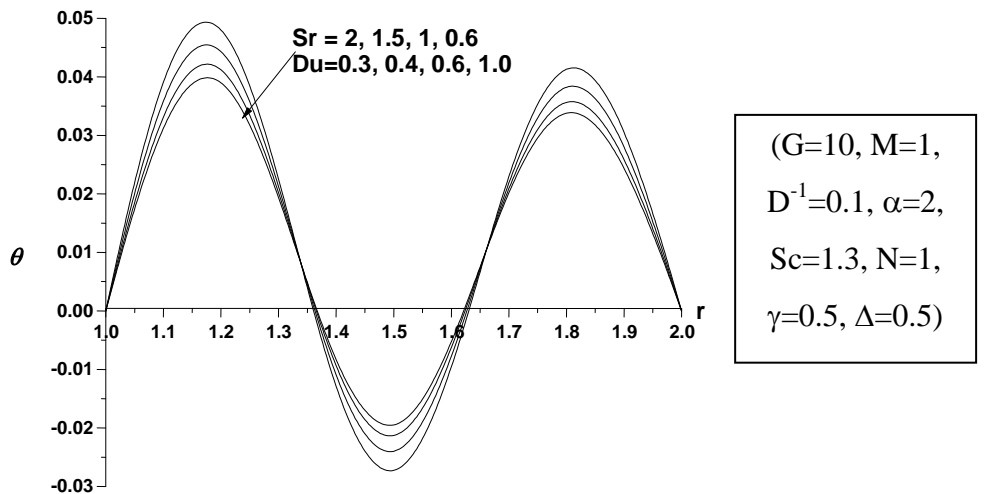Fig. 16: Variation of temperature θ with Chemical reaction parameter γ

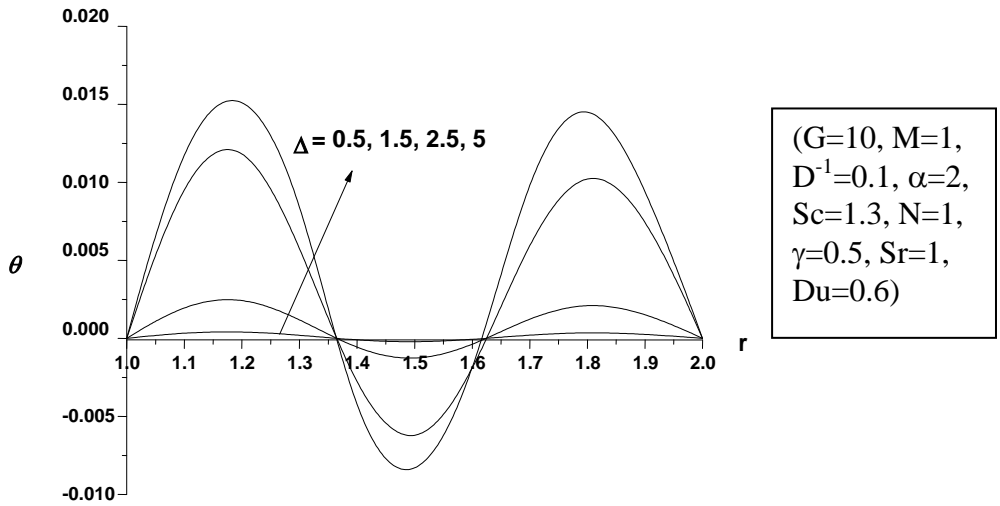Fig. 17: Variation of temperature θ with Soret and Dufour Sr/Du

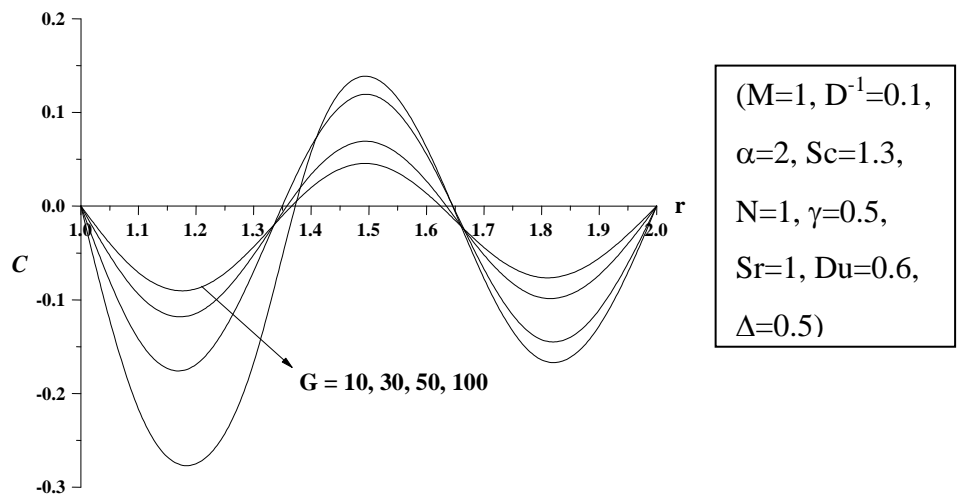Fig. 18: Variation of temperature θ with Forchheimer number Δ

Fig. 19: Variation of concentration *C* with Grashof number G

Fig. 20: Variation of *C* with M

CONFERENCE PAPER
National Conference dated 27-28 July 2017 on
Recent Advances in Graph Theory and its Applications (NCRAGTA2017)
Organized by Dept of Applied Mathematics
Sri Padmawati Mahila Vishvavidyalayam (Women's University) Tirupati, A.P.,
India
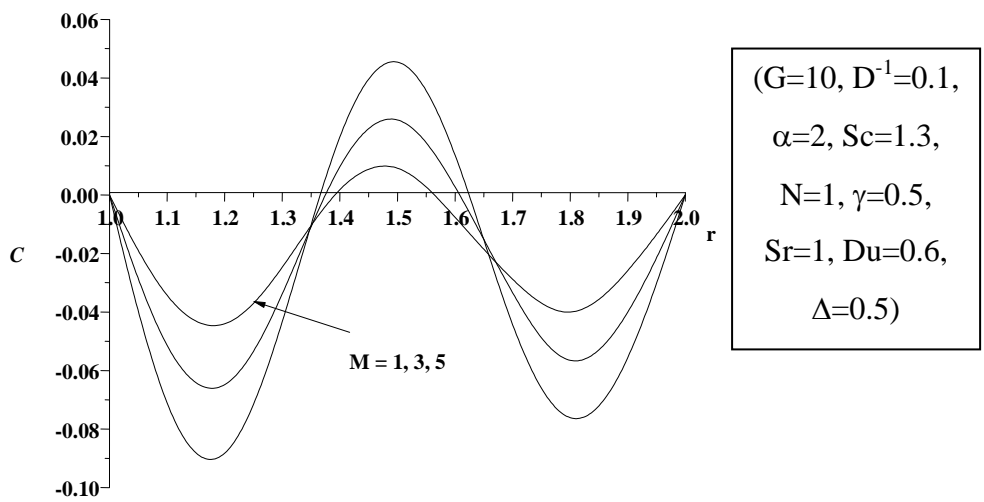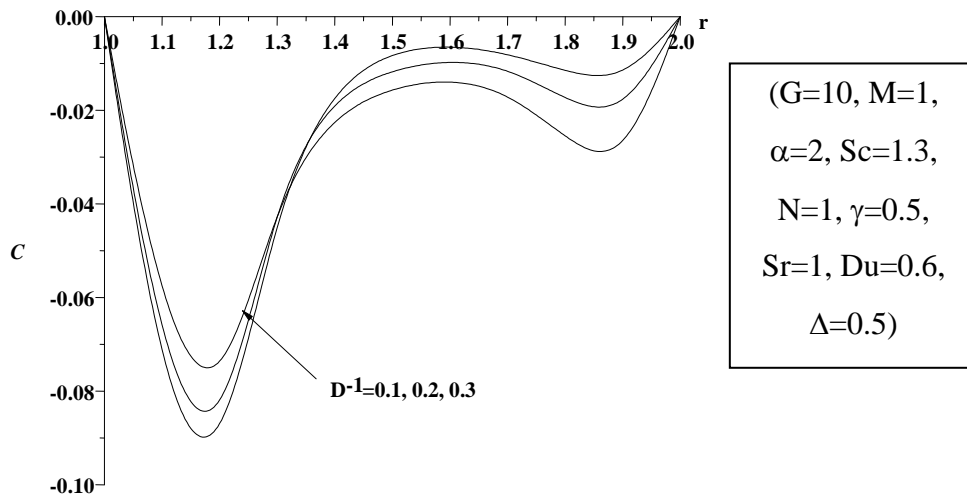
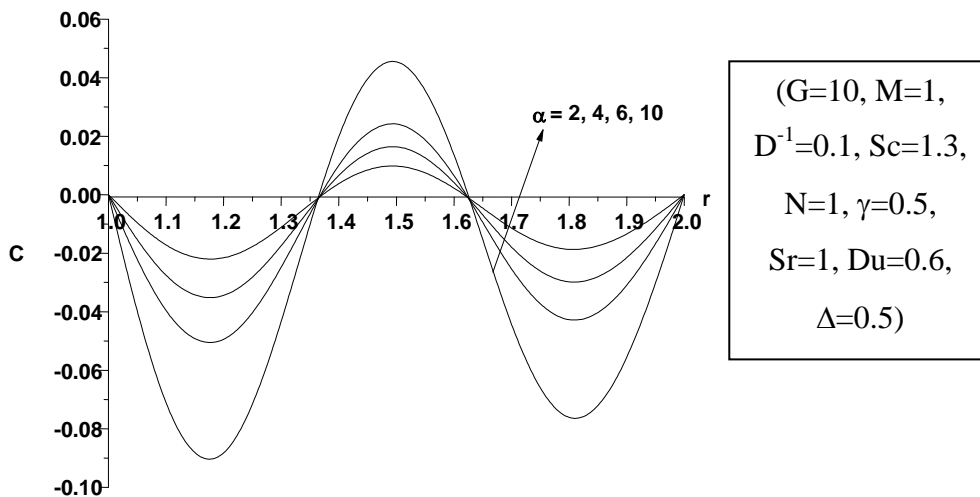Fig. 21: Variation of concentration C with Darcy parameter D^{-1}

Fig. 22: Variation of concentration C with Heat source parameter α
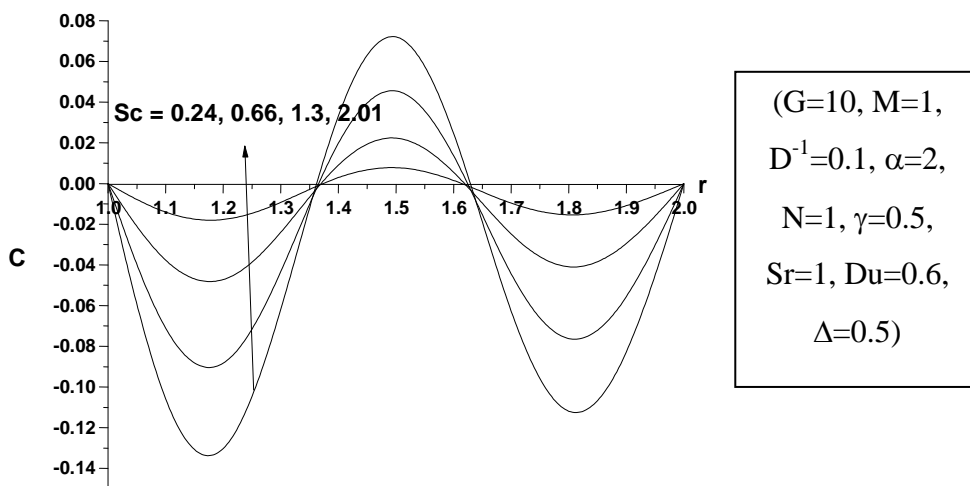
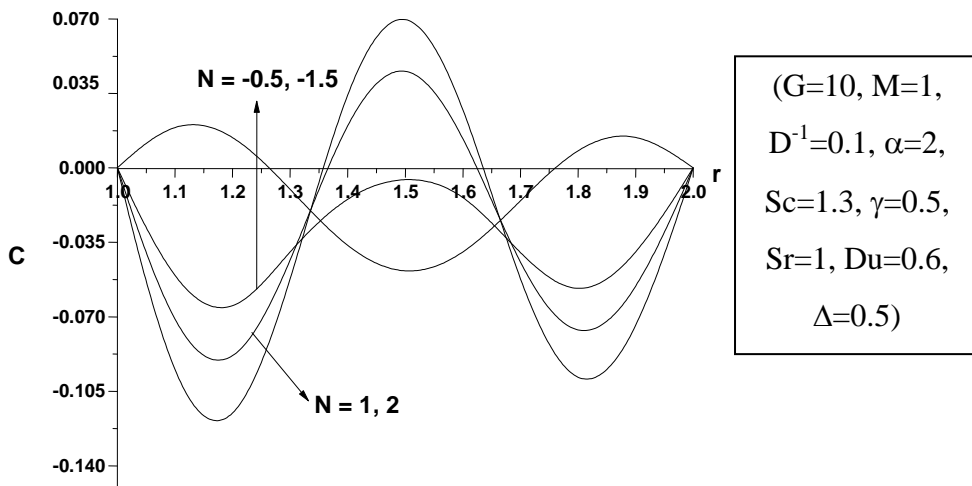Fig. 23: Variation of concentration C with Schmidt number Sc

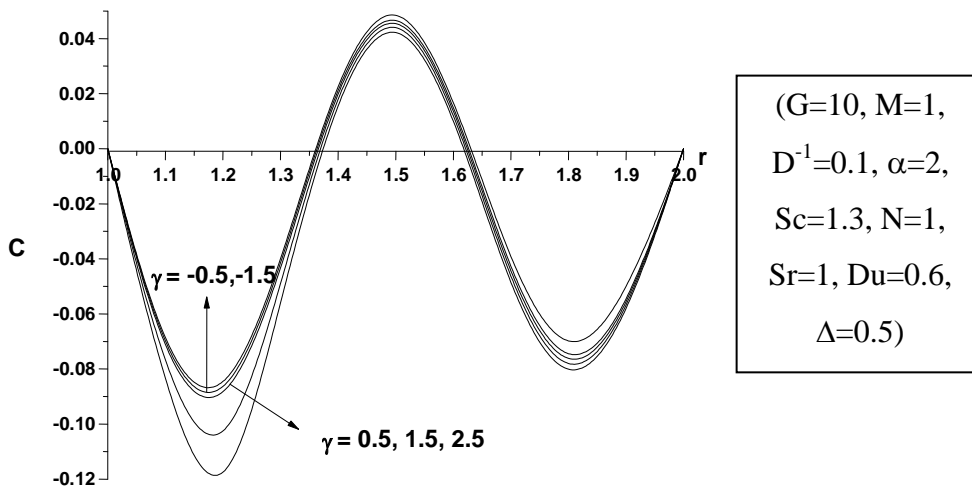Fig. 24: Variation of concentration C with Buoyancy ratio N

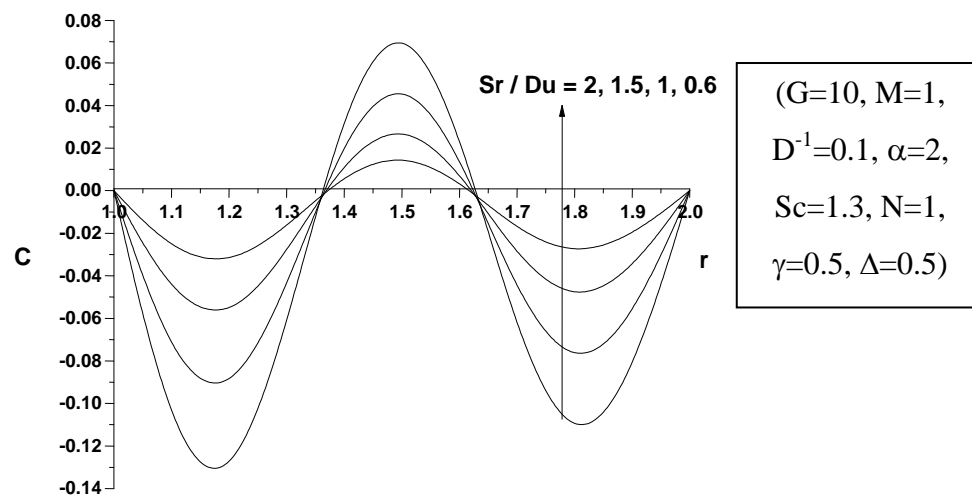Fig. 25: Variation of concentration C with Heat source parameter γ

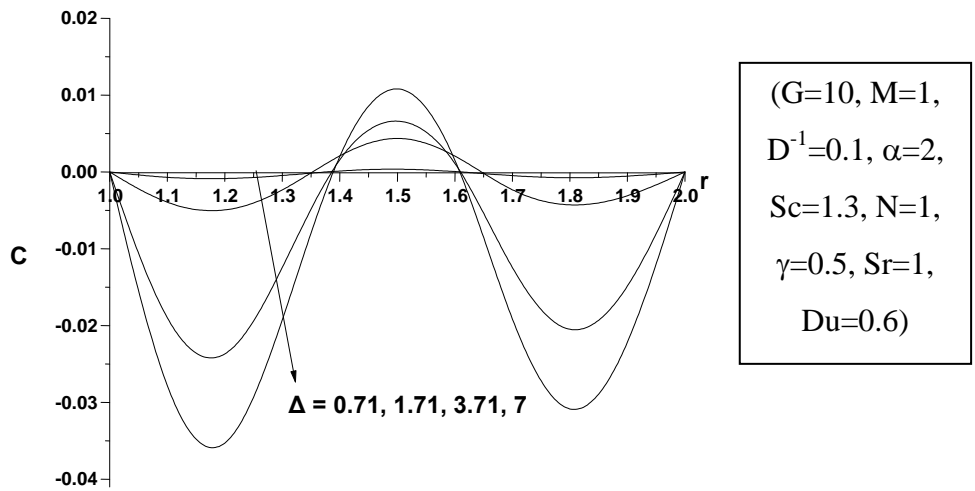Fig. 26: Variation of concentration C with Soret and Dufour Sr/Du

Fig. 27: Variation of concentration C with Forchheimer parameter

TABLE:

	$\tau(1)$	$\tau(2)$	Nu(1)	Nu(2)	Sh(1)	Sh(2)
G	0.04056	-0.02965	0.00555	-0.00398	-0.01156	0.00829
	0.04197	-0.02973	0.00569	-0.00403	-0.01176	0.00835
	0.04225	-0.02994	0.00573	-0.00406	-0.01184	0.00843
M	0.04056	-0.02965	0.00555	-0.00441	-0.01156	0.00829
	0.03648	-0.02539	0.00494	-0.00344	-0.01024	0.00716
	0.03055	-0.02061	0.00413	-0.00278	-0.0086	0.00584
D^{-1}	0.04056	-0.02965	0.00555	-0.00441	-0.01156	0.00829
	-0.00548	0.00113	0.00457	-0.2345	-0.01567	0.00657
	0.00978	-0.00824	0.00133	-0.00112	-0.00273	0.00229
α	0.04046	-0.01965	0.01555	-0.00241	-0.01356	0.00729
	0.10123	-0.06178	0.0409	-0.02288	-0.06518	0.04912
	0.22649	-0.12218	0.17335	-0.11692	-0.32564	0.23465
	0.45211	-0.30682	0.63995	-0.44624	-1.22738	0.87661
N	0.04056	-0.02965	0.00555	-0.00441	-0.01156	0.00829
	0.04253	-0.03015	0.00576	-0.00408	-0.01191	0.00847
	0.03986	-0.02816	0.0054	-0.00381	-0.01117	0.00792
	0.03889	-0.02743	0.00527	-0.00371	-0.01091	0.00772
Sc	0.04048	-0.02862	0.00681	-0.00481	-0.00257	0.00182
	0.0409	-0.02893	0.00627	-0.00444	-0.00657	0.00466
	0.04156	-0.02965	0.00554	-0.44124	-0.01156	0.00829
γ	0.04056	-0.02965	0.00555	-0.00441	-0.01156	0.00829
	0.04143	-0.02933	0.00558	-0.00394	-0.01182	0.00839
	0.04141	-0.02931	0.00564	-0.00399	-0.01142	0.00809
	0.0414	-0.0293	0.00566	-0.00401	-0.01124	0.00796
Sr/Du	0.04171	-0.02954	0.00525	-0.00371	-0.01435	0.01018
	0.04138	-0.02929	0.00519	-0.00367	-0.01077	0.00765

0.04106	-0.02905	0.00511	-0.00361	-0.00726	0.00515	
Δ						
0.04056	-0.02965	0.00555	-0.00441	-0.01156	0.00829	
0.10133	-0.07178	0.0309	-0.02188	-0.06218	0.04412	0.22849
-0.16218	0.16335	-0.11592	-0.32464	0.23065	0.45911	-0.32682
0.61995	-0.44124	-1.22638	0.87361			

VIII. CONCLUSIONS:

The coupled equations governing the flow, heat and mass transfer have been solved by using Galerkin finite method with quadratic approximation functions. The velocity, temperature and concentration have been analyzed for different parametric variations. The important conclusions of the analysis are

- An increase in Grashof number G enhances the velocity u. The temperature θ increases except in the central region while the concentration C enhances in the central region. The skin friction, the rate of heat and mass transfer increases with G on the cylinders.
- Higher the Lorentz forces smaller the velocity u. The temperature θ enhances and the concentration C reduces in the central region. The skin friction, the rate of heat and mass transfer reduces on the cylinders with increase in M.
- The velocity u reduces, the temperature θ enhances and the concentration C reduces in the central flow region with increase D^{-1}.The skin friction, Nusselt number and Sherwood number reduces with increasing D^{-1}.
- When the molecular buoyancy force dominates over the thermal buoyancy force the velocity u and temperature θ enhances irrespective of the directions of the forces. The concentration C enhances with N>0 and reduces with N <0 in the central region. The Nusselt number increases on the inner cylinder and reduces on the outer cylinder with N>0 while Nu reduces with N on r=1&2. The rate of mass transfer enhances with N>0 and reduces with N<0 on both the cylinders.
- With respect to Schmidt number Sc, we find that lesser the molecular diffusivity larger the velocity u. With increase in Sc, the temperature θ and concentration C enhances in the central flow region and reduces in the remaining region. The skin friction and Sherwood number enhances on both the cylinders. The rate of heat transfer reducers on both the cylinders with increasing Sc.
- Increasing Soret parameter (or decreasing Du) enhances the velocity u. The temperature θ enhances and the concentration C reduces in the regions adjacent to the cylinders. The skin friction, Nusselt number and Sherwood number enhances on the cylinders with increasing Sr(or decreasing Du).
- With reference to the chemical reaction parameter(γ), we find that the velocity u increases, temperature θ and concentration C decreases in the flow region in the degenerating chemical reaction case while in the generating chemical reaction case a reversed effect is noticed. The skin friction, Nusselt number and Sherwood number enhance in the degenerating chemical reaction case while in generating case a reversed effect is noticed on the cylinders.

IX. REFERENCES:

[1]. Adrian Postelnicu: Influence of magnetic field on heat and mass transfer by natural convection from vertical surfaces in porous media considering Soret and Dufour effects. Int. J. of Heat and Mass Transfer, V.47, pp.1467-1472 (2004).

[2]. Sreevani M: Mixed convective heat and mass transfer through a porous medium in channels with dissipative effects, Ph.D thesis, S.K.University, Anantapur, India (2003).

[3]. Barletta, A: Laminar mixed convection with viscous dissipation in a vertical channel. Int. J. Heat Mass Transfer, V.41, PP.3501-3513 (1998).

[4]. Zanchini E: Effect of viscous dissipation on mixed convection in a vertical channel with boundary conditions of the third kind, Int. J. Heat mass transfer, V.41, pp.3949-3959 (1998).

[5]. Indudhar Reddy, M, Narasimha Rao, P and Prasada Rao, D.R.V: Effect of Quadratic density-temperature variation on unsteady convective heat and mass transfer flow in a vertical channel. J. Pure & Appl. Phys., V.23, No.2, pp.175-187 (2011).

[6]. Madhusudhan Reddy, Y, Prasada Rao, D.R.V: Effect of thermo diffusion and chemical reaction on non-darcy convective heat & mass transfer flow in a vertical channel with radiation. IJMA, V.4, pp.1-13 (2012).

[7]. Kamalakar,P.V.S Prasada Rao,D.R.V and Raghavendra Rao,R: Finite element analysis of chemical reaction effect on Non-Darcy convective heat and mass transfer flow through a porous medium in a vertical channel with heat sources., Int.J.Appl.Math and Mech, V-8(13), pp.13-28(2012).

[8]. Rajasekhar, N.S, Prasad, P.M.V and Prasada Rao, D.R.V: Effect of Hall current, Thermal radiation and thermo diffusion on convective heat and mass transfer flow of a viscous, rotating fluid past a vertical porous plate embedded in a porous medium. Advances in Applied Science Research, V.3, No.6, pp.3438-3447 (2012).

[9]. Muthucumaraswamy, R , Dhanasekhar, N and Eswar Prasad, G: Rotation effects on flow past an accelerated isothermal vertical plate with chemical reaction of first order. IJMA, V.3, No.5, pp.2122-2129 (2012).

[10]. Jafarunnisa, S: Transient double diffusive flow of a viscous fluid with radiation effect in channels/Ducts, Ph.D Thesis, S.K.University, Anantapur, India (2011).

[11]. Alam, Md, Delower Hossain, M and Arif Hossain, M: Viscous dissipation and joule heating effects on steady MHD combined heat and mass transfer flow through a porous medium in a rotating system. Journal of Naval Architecture and Marine Engineering, V.2, pp.105-120 (2011).

[12]. Kafoussias N G, Williams EW (1995): Thermal-diffusion and diffusion-thermo effects on mixed free-force convective and mass transfer boundary layer flow with temperature dependent viscosity. *Int J EngSci*33, 1369-84.

[13]. Alam, M.S., Rahman, M. M., Abdul Maleque M. (2005): Local Similarity solutions for unsteady MHD free convention and mass transfer flow past an impulsively started vertical porous plate with Dufour and Soret effects. *Thammasat Int J Sci Tech* 10, 1-18.

[14]. Alam, M.S., Rahman, M.M., Samad M A (2006): Dufour and Soret effects on unsteady MHD free convection and mass transfer flow past a vertical porous plate in a porous medium. *Non-linear Anal Model Contr*, 11, 217-226.

[15]. Lakshminarayan P A, Sibanda, (2010): Soret and Dufour effects on free convection along vertical wavy surface in a fluid saturated darcy porous medium. *Int. J. of Heat and Mass Transfer* 53, 3030-3034.

[16]. Naga Radhika V, Prasad Rao D R V (2010): Dissipative and radiation effects on heat transfer flow of a viscous fluid in a vertical channel. *J. of Pure and Applied Phy.* 22(2), 255- 267.

[17]. Dulal pal, Hiranmoy Mondal (2011): Effect of Soret, Dufour, chemical reaction and thermal radiation on MHD, non-darcy, unsteady mixed convective heat and mass transfer over stretching sheet. *Common Non-linear Sci Number Simulat* 16, 1942-1958.

[18]. Ching-Yang-Cheng (2011): Soret and Dufour effects on free convective boundary layer over inclined wavy surface in a porous medium. *Int. Communications in Heat and Mass Transfer* 38, 1050-1055.

[19]. Dulal pal, Hiranmoy Mondal (2012): Effects on MHD non-darcian mixed convective heat and mass transfer over a stretching sheet with non-uniform heat source/sink. *Physica B* 407 642-651.

[20]. Sulochana.c, Tayappa.H: Finite element analysis of thermo-diffusion and diffusion- thermo effects on combined heat and mass transfer flow of viscous, electrically conducting fluid through a porous medium in vertical channel, Int . J. mathematical achieves – 5(9), 2014, PP:1-13.

[21]. Ramana Reddy, J.V., Sugunamma,V., Sandeep, N., Mohan Krishna, P. (2014): Thermal diffusion and chemical reaction effects on unsteady MHD dusty viscous flow. *Advances in Physics Theories and Applications*38, 7-21.

[22]. Raju, C.S.K, Sandeep, N., Sulochana, C., Sugunamma, V., Jayachandra Babu, M. (2015): Radiation, Inclined Magnetic field and Cross-Diffusion effects on flow over a stretching surface. *Journal of Nigerian Mathematical Society (In Press)*

[23]. Raju, C.S.K., Sandeep, N., Jayachandra Babu,M., Sugunamma, V., (2015): Radiation and chemical reaction effects on thermo-phoretic MHD flow over an aligned isothermal permeable surface with heat source.

[24]. Raju, C. S. K., Jayachandra Babu, M., Sandeep, N., Sugunamma, V., Reddy, J.V.R (2015): Radiation and soret effects of MHD nano-fluid flow over a moving vertical plate in porous medium, *Chemical and Process Engineering Research* 30, 9-23.

[25]. Leppinen,D.M.,Pop,I.Rees,D.A and Storesletten,L: Free convection in a shallow annular cavity filled with a porous medium., J.Porous Media,V.7,pp.929-938(2004).

[26]. Jha,B.K: Free convection flow through an annular porous medium., heat Mass Transfer,V.41,pp.675-679(2005).

[27]. Saravannan,S and Kandaswamy,P: Non-darcian thermal stability of a heat generating fluid in a porous annulus., Int.J.Heat Mass transfer,V.46,pp.4863- 4875(2003).

[28]. Charrier-Mojtabi,M.C: Numerical simulation of two and three dimensional free convection flows in a horizontal porous annulus using a pressure and temperature formulation., Int.J.Heat Mass Transfer,v.40,pp.1521-1533(1997).

[29]. Chmaissem,W.,Suh,S.J.,Degueene,M; Numerical study of Boussinesq model of natural convection in an annular space: Having a horizontal axis by circular and elliptical isothermal cylinders, Appl. Thermal eng.,V.22,pp.1013-1025(2002).

[30]. SivanJaneya Prasad, P: Effects of convection heat and mass transfer in unsteady hydro magnetic channels flow. Ph. D thesis S.K. University, Anantapur, India (2001).

[31]. Neeraja G: Ph. D thesis, S.P. Mahila University, Tirupathi, India (1993).

[32]. Antonio Barletta: Combined forced and free convection with viscous dissipation in a vertical duct, Int. J. Heat and mass transfer v. 42, pp. 2243–2253 (1999).

[33]. Shaarawi, EL. M.A. I and AL. Nimir, M.A: Fully developed laminar natural convection in open ended vertical concentric annuli, Int. J. Heat and mass transfer pp. 1873–1884 (1999).

[34]. Al. Nimir, M.A: Analytical solutions for transient laminar fully developed free convection in vertical annuli, Int. J. Heat and mass transfer, v. 36, pp. 2388–2395 (1993).

[35]. Chamkha, A. J., EL-Kabeir, S. M. M., and Rashad, A. M., Heat and mass transfer by non-Darcy free convection from a vertical cylinder embedded in porous media with a temperature dependent viscosity, Int. J. Number. Methods Heat Fluid Flow, V. 21, No. 7, pp. 847–863(2011).

[36]. Prasad, M.V.S.N: Hydro-magnetic mixed convective heat and mass transfer flow through a porous medium in channels, pipes with heat sources. Ph.D Thesis, S.V.University, Tirupati, pp: 73-93 (2009).

[37]. Sreenivas Reddy, B: Thermo-diffusion effect on convection heat and mass transfer through a porous medium, Ph. D thesis S.K. University, Anantapur, India (2006).

[38]. Sudheer Kumar, Dr.M.P. Singh, Dr Rajendra Kumar: Radiation effect on natural convection in porous media; Acta Ciencia Indica v. XXXII M. No.2, (2006).

[39]. Padmavathi, A: "Finite element analysis of Non-Darcian convective heat transfer through a porous medium in cylindrical & rectangular ducts with heat generating sources and radiation" "Ph. D thesis, S.K. University Anantapur, India (2009).

[40]. Madhusudha Reddy,P: Mixed convective heat and mass transfer flow through a porous medium in channel with Radiation effect. Ph. D. Thesis (2010).

[41]. Sudarsana Reddy,P, Sreenivas,G, Sreenivasa Rao,P and Prasada Rao, D.R.V: Non-Darcy mixed convective heat and mass transfer flow of a viscous electrically conducting fluid through a porous medium in a circular annulus in the presence of temperature dependent heat sources with Soret and Dufour effects-A-finite element study., Int.J.Comp and Appl.Math, V,.5(5),pp.595-609(2010).

[42]. Sudarsana Reddy.P, and Prasada Rao, D.R.V: Combined influence of Soret and Dufour effects on convective heat and mass transfer flow through a porous medium in cylindrical annulus with heat sources., African Journal of Mathematics and Computer Science Research Vol. 3(10), pp. 237-254, 2010.

[43]. Mallikarjuna,B, Ali. J. Chamkha and R,Bhuvana Vijaya: Soret and Dufour effects on double diffusive convective flow through a non-Darcy porous medium in a cylindrical annular region in the presence of heat sources., J. Porous Media,V.17(7), pp.623-636(2014).

[44]. Sreenivas Reddy, B: Thermo-diffusion effect on convection heat and mass transfer through a porous medium, Ph. D thesis S.K. University, Anantapur, India (2006).

[45]. Sulochana,c and Tayappa,H: Non-darcy convective heat and mass transfer flow in a circular annulus with Soret, Dufour effects and constant heat flux, Int.J.Scintific and Innovative Mathematical research, V.2(8), 2014, pp.684-697.

[46]. Tao, L. N: On combined and forced convection in channels, ASME J. Heat Transfer, V.82, pp.233-238(1960).

[47]. Neeraja,G: Effect of Thermo-Diffusion on Mixed Convective Heat and Mass Transfer Flow in a Circular Annulus with Heat Sources and Chemical Reactions, Advances in Physics Theories and Applications, 2016.